FINAL REPORT

OCTOBER 1967

COMPUTER SIMULATION OF AUTOMATIC IMAGE REGISTRATION PERFORMANCE

☐ SECRET ☐ CONFIDENTIAL ☐ UNCLASSIFIED

CONTRACT INSPECTION REPORT

CONTRACT NO.	TASK NO.
TO:	DATE
	INSPECTION REPORT NO. *(If final, so state)*
	ESTIMATED COMPLETION DATE
NAME OF CONTRACTOR	
TYPE OF COMMODITY OR SERVICE	
THE CONTRACTOR IS ON SCHEDULE ☐ YES ☐ NO	THE CONTRACTOR WILL PROBABLY REMAIN WITHIN ALLOCATED FUNDS ☐ YES ☐ NO IF ANSWER IS "NO" ADVISE RECOMMENDATION AND/OR ACTION OF SPONSORING OFFICE, ON REVERSE HEREOF. IF KNOWN, INDICATE MAGNITUDE OF ADDITIONAL FUNDS INVOLVED.
PER CENT OF WORK COMPLETED - PER CENT OF FUNDS EXPENDED -	

HAS AN INTERIM REPORT, FINAL REPORT, PROTOTYPE, OR OTHER END ITEM BEEN RECEIVED FROM THE CONTRACTOR DURING THE PERIOD? ☐ YES ☐ NO *(If yes, give details on reverse side.)*

HAS GOVERNMENT-OWNED PROPERTY BEEN DELIVERED TO CONTRACTOR DURING THIS PERIOD? ☐ YES ☐ NO *(If yes, indicate items, quantity, and cost on reverse side.)*

INCENTIVES

IS THIS AN INCENTIVE CONTRACT ☐ YES ☐ NO

IF YES, CHECK TYPE

☐ COST ☐ AWARD FEE ☐ PERFORMANCE ☐ DELIVERY

NOTE:
USE REVERSE SIDE FOR COMMENTS.
FINAL REPORT MUST CONTAIN INCENTIVE EVALUATION.

OVERALL PERFORMANCE OF CONTRACTOR

1. ☐ OUTSTANDING
2. ☐ EXCELLENT
3. ☐ VERY GOOD
4. ☐ ABOVE AVERAGE
5. ☐ AVERAGE
6. ☐ MINIMUM ACCEPTABLE
7. ☐ UNSATISFACTORY

IF OVERALL PERFORMANCE OF CONTRACTOR IS UNSATISFACTORY OR MINIMUM ACCEPTABLE INDICATE REASONS ON REVERSE SIDE.

RECOMMENDED ACTION

☐ CONTINUE AS PROGRAMMED

☐ WITHHOLD PAYMENT PENDING SATISFACTORY PERFORMANCE

☐ CLOSE OUT

☐ OTHER *(Specify)*

IF THIS IS A FINAL REPORT PUT COMMENTS ON REVERSE IN NARRATIVE FORM ON CONTRACTOR'S PERFORMANCE AND CERTIFY THAT ALL DELIVERABLE ITEMS UNDER THE CONTRACT HAVE BEEN RECEIVED. THESE INCLUDE, WHERE APPLICABLE, THE FOLLOWING:

ITEM	REC'D	DOES NOT APPLY	ITEM	REC'D	DOES NOT APPLY
PROTOTYPES			MANUALS		
DRAWINGS AND SPECIFICATIONS			FINAL REPORT		
PRODUCTION AND/OR OTHER END ITEMS			SPECIAL TOOLING		
			OTHER GOVERNMENT PROPERTY		

DATE OF LAST CONTACT WITH CONTRACTOR

SIGNATURE OF INSPECTOR	DIVISION
INSPECTOR'S EXTENSION	SIGNATURE OF APPROVER

FORM 12-67 1897 USE PREVIOUS EDITION

☐ UNCLASSIFIED ☐ CONFIDENTIAL ☐ SECRET (12-36)

NARRATIVE REPORT ☐ INTERIM ☐ FINAL

Excel - 10
Good - 9
Above Avg - 8
Avg 7
Marginal 6

Conf: ± 2%

Perf: ± 2%

1 February 1967

~~POSSIBLE~~ TEST PROGRAMS

There are a number of subjects worthy of investigation that were not specifically mentioned in the proposed Phase II program. We feel that a study of each of these subjects as soon as possible will be of considerable benefit to the development of the Automated Stereo Scanner.

Five such subjects are listed below, each with the proposed level of effort, a short description of the subject and the proposed work, an indication of relative importance to the scanner program, and an approximate cost. In each case the proposed work is not an exhaustive study, but rather just enough work to determine a qualitative measure of potential problems and solutions, and to prepare a report on the findings. It is assumed that longer term or extensive studies would more properly be the subject of a stereo scanning research program.

1. Distortion Feedback Servo Loop Stability

We propose to use the existing PDP-1 scanner and distortion detection programs, augmented by a program to insert a feedback connection to the scanner based on the detected distortions. This will enable us to study the conditions under which the system will converge to correct image distortion and those in which it becomes unstable. The advantages of such an approach to this problem are the ability to slow down the operation to see what goes on, and to separate and control the system variables.

The PDP-1 system is not a perfect analog of the Stereo Scanner system, but it is expected that it is close enough to provide a qualitative comparison. This program would be for one programmer over a three month period, plus supervision and discussions with various staff members. The computer and its maintenance are not charged to the program. The relative importance of

this program is high. The approximate cost [redacted] STAT

2. Registration Correction Accuracy ✓

It is proposed that the EROS unit be used to make measurements of the ability of the automatic detection and correction logic to register two images as compared to the registration made by an operator using "floating marks" with the same instrument operating manually. It is proposed that differences between settings be measured rather than absolute parallaxes, and that no attempt be made to make measurements in the micron range.

In order to make the tests it will be necessary to modify EROS so as to enable marks to be projected onto the object stages. Initial tests will be done with identical images, simulating no relief, in order to remove biases and to check the effects of image content and contrast. Further tests will be made with true stereo of varying relief. These tests will check the effect of variations of relief within the field of view.

The level of effort consists of specifying the mark projectors and how they are to be inserted in EROS, making these additions to EROS, conducting the tests, and reducing the data. This is approximately one month of technician work and two months of an engineer. The relative importance of the work is medium, and the approximate cost is about [redacted] STAT

3. Image Dissector Scan Distortion ✓

It has been recently pointed out that there may be several advantages to providing a two-loop servo system in the stereo scanner, namely that the detected distortions be used to distort the electronic scanning raster on the image dissectors. The resultant scanning raster distortions are sent to the optical-mechanical servo motors as error signals. In this way the electronic loop can accomodate rapid changes and can operate in rectilinear

coordinates. The opto-mechanical servo will operate in polar coordinates and will act as the integrating element in the system. A definite potential advantage is that the signals delivered to the mechanical servos will be true error signals unaffected by image content. This will be a big help in the derivation of the anamorph drive signals.

We propose to set up a pair of image dissectors and test them in a closed loop system, providing for raster distortion. The equipment set up will be similar to that used for the vidicon tests except that additional circuitry must be added to provide for scan distortion.

The level of effort would be one engineer for two months and one technician for three months. The material costs should be less than [ ] STAT assuming that the image dissectors are purchased as a part of Phase II. This labor includes a lot of the image dissector tests already planned for Phase II. The costs in addition to the already planned Phase II costs, STAT would amount to about [ ] We believe this work to be of relatively high importance.

4. Custom Design of First Relay Lens

We propose that a study be directed toward the feasibility of procuring a custom made lens for the first relay lens used in the rhomboid arms. The program would be to have a lens designer look at the problem and give an opinion of the likelihood of performance improvement with a custom design. If the answer is yes, we propose that such a lens be designed and that a quotation be obtained for the fabrication of three such lenses (one spare). This is a six to eight week task of one engineer about 3/4 time. The cost STAT would be approximately [ ] and possibly less. This is a medium priority task.

5. Zoom Lens Survey

We propose, as a result of our tests on the Angenieux lens, to rent and test such other high performance zoom lenses as are obtainable. The manufacturer data on such lenses is inadequate for our purposes and in some cases it is overly optimistic and somewhat misleading. The level of effort is one engineer for four days per lens, plus a day of technician time per lens. Assuming that six such lenses might be obtained at an average rental

STAT [ ] then the total cost of these tests would be about

STAT [ ]. These tests are of medium relative importance.

STAT

FINAL REPORT

OCTOBER 1967

COMPUTER SIMULATION OF AUTOMATIC IMAGE REGISTRATION PERFORMANCE

STAT

STAT

TABLE OF CONTENTS

Section 1

INTRODUCTION

A.S.S.

1.0 INTRODUCTION

The registration of photographic images is basic in practically all photogrammetric operations, and in the process of stereo photo-interpretation. Several instruments have been built by [redacted] utilizing electronic scanning techniques to provide information to a system for removing parallaxes. STAT

The purpose of this project has been to simulate the scanning and correlation technique described below with the aim of evaluating its abilities and suggesting methods for improvement. In order to do this, the PDP-1 computer has been programmed and its associated precision CRT scanning system set up so as to match the hardware system as closely as possible. Figure 1 shows the PDP-1 computer's display tube, and on the right, the precision scanner.

The heart of any automatic registration instrument is the correlation system. Parallaxes are usually detected by noting the difference in arrival times between corresponding portions of the two channels of video signals generated by a TV camera system or a Flying Spot Scanner System. The output signals from the parallax analyzer have a magnitude and polarity that are dependent upon the magnitude and direction of the parallax between the left and right images at any instant.

In the system being simulated, the video signals are generated by a pair of image dissector tubes and converted to binary waveforms by a peak and valley (inflection) detector. The binary signals are then processed by the "summation of disagreements" technique described below and the integrated error signals fed back to distort the scans on the image dissectors until no parallax errors are detected.

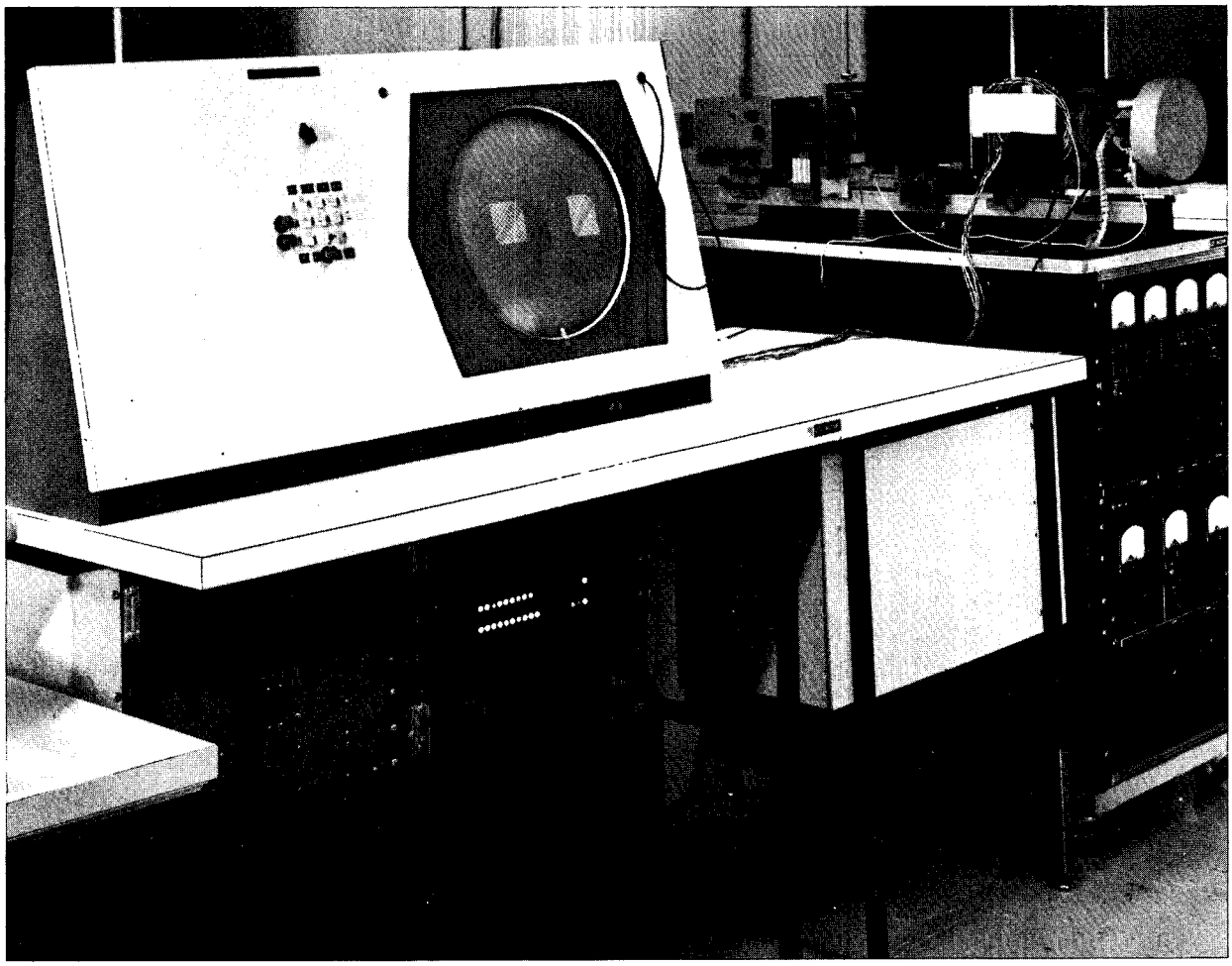

Fig. 1 - PDP-1 Scanner

1.1 Summation of Disagreements

Parallax discriminations proceed as follows:

A. The two binary video waveforms are compared; if the levels disagree then an add pulse or a subtract pulse is forwarded to a summation counter for each increment of disagreement. ?

B. If the right video initiated the disagreement, then an add pulse is forwarded. ?

C. If the left video initiated the disagreement, then a subtract pulse is forwarded.

D. If the video levels change together, then the process is continued as before the changes.

This technique can be applied to the video data as they are generated, ? and only one memory bit is required to remember which waveform changed last.

The outstanding feature of this technique is that there are no inherent pull-in range limitations. If the video signal is made up of low frequencies undistorted by harmonics or other high frequencies, the pull-in range should be almost equal to the raster size.

Only because of the simulation technique? Or will it be true in actual system? NO

Section 2

GENERAL DESCRIPTION

2.0 GENERAL DESCRIPTION

The first part of the project was concerned with writing the computer programs necessary to do the simulation. The second part has been the performance of an extensive series of tests in which parameters relating to the hardware system have been determined, and the limitations of the system defined.

Since the digital computer performs operations serially rather than in parallel, there are necessarily some differences between the "hardware system" and the "software simulation". In the simulation a complete scan is generated and the inflection signals stored for processing. The processing consists of comparing the streams of inflection signals from the left and right scans against each other and against reference signals to determine the direction of the scan when a disagreement occurred. These disagreement counts are steered by the reference signals to accumulators which store the sign and magnitude of the X and Y translation, scale and skew components. These six counts, properly scaled, are used in the generation of the next scan in such a way as to attempt to reduce the counts in that cycle. The process is ended when the average of the counts drops below a selected limit.

The "hardware system" contains integrators corresponding to the accumulators for each of the error components. Feedback from these integrators to the scan generation circuitry is on a continuous basis rather than a sampled basis and acts so as to alter the scan to try to reduce the inputs to the integrator to zero.

Another major difference is that the hardware system is limited by overloading of the integrators while the simulator system is limited by overlapping or wrap-around on the CRT scanner, a condition in which the scan raster goes off one edge of the tube and appears on the opposite side.

2.1 Program Description

There are two main routines in the computer program used to simulate the closed loop scanning and distortion correction system. The first of these routines was developed under the Digital Mapping System and consists of a program to generate and store all the cathode-ray tube coordinate locations for a pair of crossed diagonal scans.

Figure 2 is a photograph of a crossed diagonal scan. The focus is set so that each of the 1152 points is discernible (each crossover represents two points). Figure 3 is a photograph of the same scan with the spot defocused to cover the area of four of the focused spots.

The computer causes the CRT to execute the two different scans (called left and right) in succession over a single image to simulate the effect of scanning a pair of images. Two scans of a single image are used to provide close control of variables. The input to the computer is the output of the video peak and valley (inflection) detectors, a binary signal ("0" or "1"), for each point, which is stored in the computer storage address from which the corresponding display point coordinate location is removed.

Following the scans, this routine performs a sum of disagreements operation (see Appendix I) on the stored data from the two scans and analyzes it to provide the sum of the six error counts - - translation, scale and skew for both X and Y as well as the inflection counts for the left and right scans. In the hardware system this would correspond to the outputs of the integrator networks.

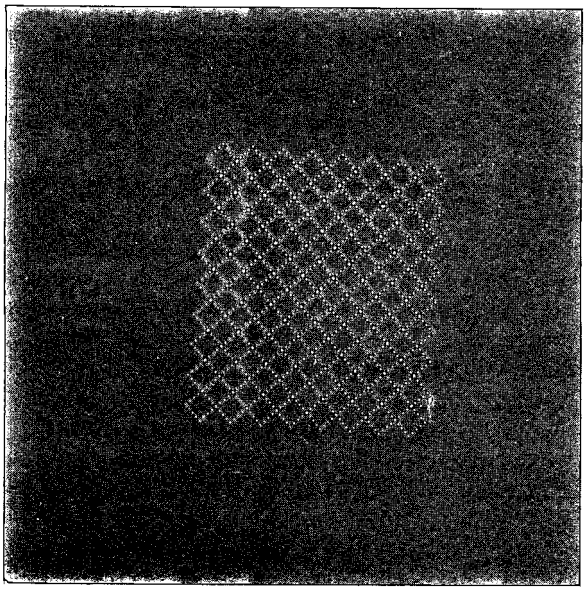

Fig. 2 - Raster with focused spot

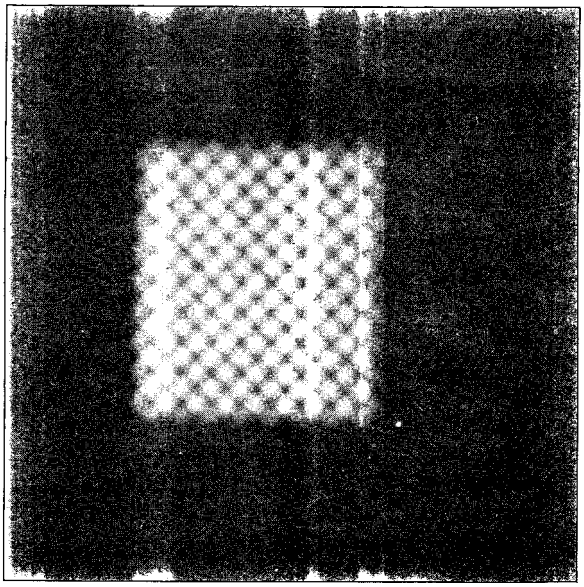

Fig. 3 - Raster with defocused spot

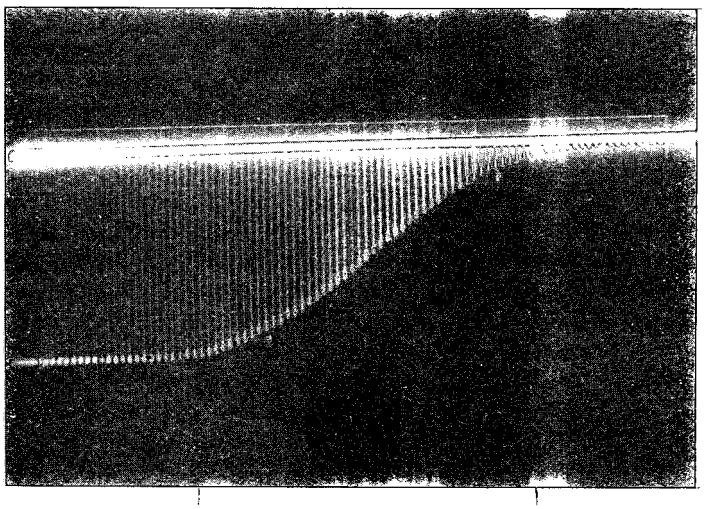

Fig. 4 - Edge response with defocused spot

The second major routine in the program has been written as a part of this project. This routine, known as FDBK61, has as its data inputs, the six error counts, the inflection counts, and the total disagreement count derived in the routine above. Using these counts the routine calculates the amounts by which the position, scale and skew of the left scan are to be changed in order to minimize the differences between left and right scans, that is, to reduce the error counts to zero.

2.2 Operator Control

Operator inputs to the program are the initial position and distortions for the left scan, and the feedback factors. The feedback factors affect the range over which these errors can be reduced and are related to the size of the steps taken between scans. These factors correspond to loop gain and bandwidth in a hardware system. The overall scale of the raster can also be controlled.

Two subroutines, also written as a part of this project, enable the operator to control the program input and the display and typewriter outputs. The first of these, the input routine, allows the operator to set or reset the initial left scan position and distortions, the right scan position and distortions and the feedback factors.

2.3 Output Capabilities

The display subroutine, generates a scan which appears on the face of the large display CRT. This display is a plot of the sign and magnitude of the six left scan deviated values as a function of the number of trials made. It can also display the total disagreement count and the left and right inflection counts as a function of the number of trials made.

The typewriter output routine enables the operator to observe, scan by scan, the position, scale and skew errors; as well as the modified values fed back from the individual error counters (integrators) which will be used to alter the left scan distortion for the next scan pair. The actual values at the error counter outputs can also be typed out, as can the total disagreement count and the left and right inflection counts.

Section 3

PRELIMINARY TEST PROGRAM

Test of PDP-1 artificial error factor

3.0 PRELIMINARY TEST PROGRAM

3.1 Focus Setting Investigations

Prior to the correlation tests it was necessary to determine the cathode-ray tube spot size relative to a standard unit of cathode-ray tube deflection. The generation of a simple line scan across a sharp edge in the image plane, and the subsequent measurement of the width of the edge in deflection steps with various focus settings accomplished this. This was done by means of the output of the scanner photomultiplier being displayed on an oscilloscope synchronized to the scanner deflection. The resultant display for a particular focus current setting was photographed, appearing as a series of pulses as shown in Figure 4. The pulses represent the photomultiplier tube output as a result of intensifying the scanner cathode-ray tube at successive scanner positions. In this case the scanner was being deflected by 2 mils, the smallest possible increment. As can be seen from the figure, the spot completely crossed the edge in about 50 deflection increments. The shape of the pulse envelope indicates that the spot is, as desired, without sharp edges. Working with spots of this type, it is more meaningful to express the spot size as the width between half power points or, for the sake of ease of measurement, as between the 15% and 85% points.

> | | | <
> 0 25 50 75 100

The measurements were made at several focus voltages and repeated for several intensity settings. Figure 5 shows the calibration curves for intensity settings of 80 and 90 volts.

From these curves, the focus setting required to give a spot diameter corresponding to 3.5 times the distance between successive sample points, for each of the raster sizes, at an optimum intensity, could be determined.

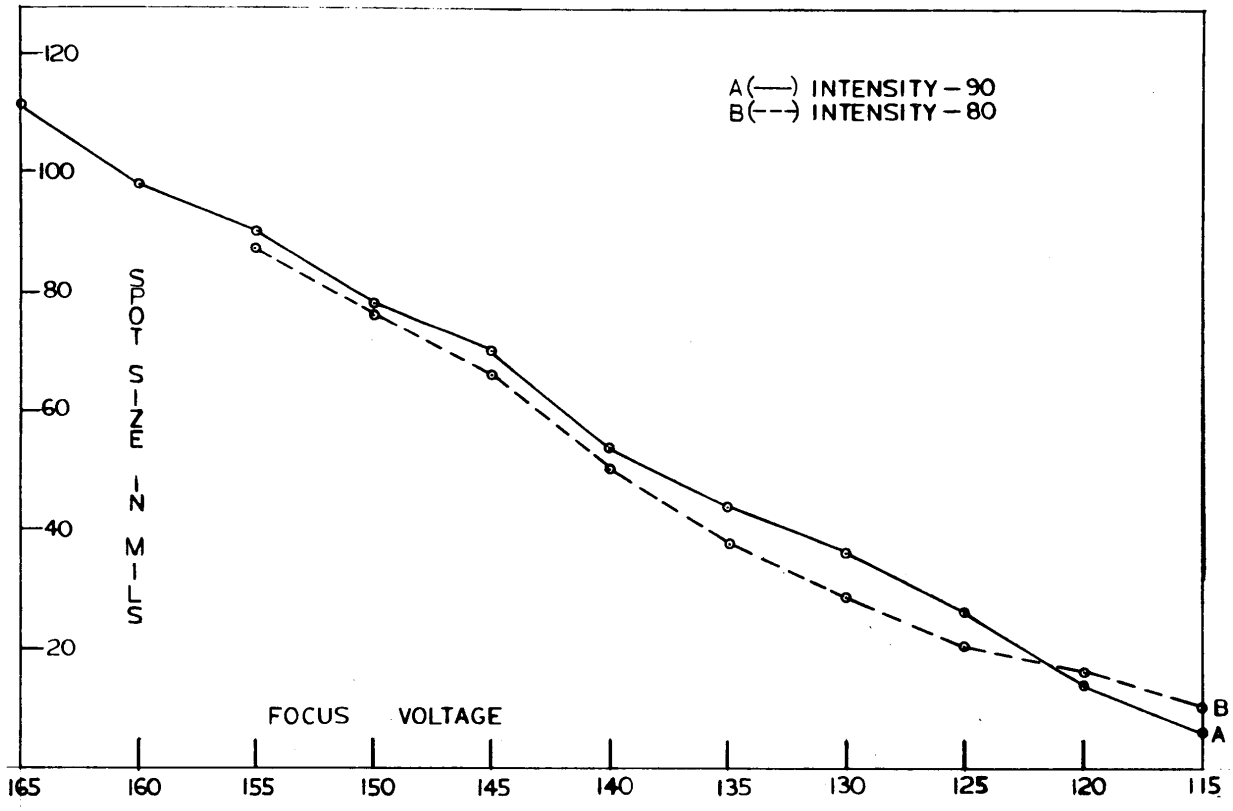

FIG-5
SPOT SIZE VS. FOCUS VOLTAGE

For a raster of gross scale 5 (approximately 1 1/4 inch square at the CRT face), the focus was set at 162 v. Gross scales of 4 and 3 (4/5 and 3/5 of the previous raster size) have corresponding focus voltages of 152 v and 142 v respectively.

Pull-in ranges for each factor independently and for combination of these factors were measured. The effects of the feedback factors and the average inflection count were investigated. The possibility of eliminating inflection counts as a feedback parameter has been examined, since the hardware system has no provisions for this type of scaling. The outcome of these tests determined relationships between the feedback and integration constants for each of the six errors, and the magnitude of the pull-in range as a percentage of the raster size for several different test samples covering a wide range of correlatable images.

3.2 Preliminary Tests

During the programming phase, several series of tests were run on samples of aerial photography to determine program behavior. With a sample of high altitude imagery containing mountain ridges, it was found that distortions ranging up to 10% of the raster size in each of the six parameters concurrently could be corrected to within 1/2%. This lower value is determined by the error limit calculation and can be reduced at the expense of number of trials.

3.2.1 Image Anisotropy Effects

Several facts were noted during these tests. The most obvious of these was the dependence of pull-in speed (number of trials necessary to reduce error to lower limit) on the direction of the image structure. That is, when the ridges ran from top to bottom in the area scanned (the Y direction) the X distortions pull in much faster than the Y distortions. When the imagery was tilted so that the ridges were at approximately 45°, X and Y pull in in equivalent steps, but not as rapidly as X had above.

3.2.2 Simultaneous Parallax and Distortion Clearance

Initially tests were run with a program which acted first to reduce X and Y translations to the error limit before acting on X and Y scale and skew. When this was altered to the program which acted on all six simultaneously, it was found that for equivalent amounts of introduced distortions, the X and Y scale and skew would act in an erratic manner until X and Y translation had been reduced to within about 3%, and then they would be reduced. For some images, however, scale and skew distortions would increase so much that the translation would not be able to correct for them and the correlation would be lost. Changing the feedback values to reduce the loop gain in the scale/skew correction loops reduced this blow-up effect, but also seems to have reduced the pull-in range. The scale and skew distortions now increase before they begin to be reduced, an effect predicted at the end of Appendix I.

3.2.3 Test Data

Tables 1 through 8 are copies of the computer typeouts from some of these test runs. The first values represent the amount of error or distortion introduced into the left raster by the programmer. For X and Y translations, these values can be divided by 340 (the number of spots in a row times the

gross scale (5)) and the result multiplied by 100 to give a direct percentage error ($\frac{EC}{340} \times 100 = \%\ E$). The scale values are normalized to a base of 256. The error count minus 256 divided by 256 and multiplied by 100 gives percentage error ($\frac{(EC - 256)}{256} \times 100 = \%\ E$).

The skew distortions combine to give a measurement of rotation. If X skew = -Y skew, the whole raster rotates evenly. Otherwise, some lines through the origin rotate more than others. The actual average rotation, and the range of rotation are both difficult to compute exactly, but we may approximate them from the counts as follows:

$$\text{Average Rotation in Degrees} = D\,\frac{28\,(Y\ \text{skew} - X\ \text{skew})}{256}$$

$$\text{Range of Rotation in Degrees} = D\,\frac{56\ \left|X\ \text{skew} + Y\ \text{skew}\right|}{256}$$

$$\text{Where}\quad D = \frac{X\ \text{scale}\ \ Y\ \text{scale}}{256 \times 256} - \frac{X\ \text{skew}\ \ Y\ \text{skew}}{256 \times 256}$$

These relationships do not include the effects from one scale being larger than the other, for then the average rotation is modifed slightly, and the range of rotation is modified considerably.

The sets of values below the first set in each table are the error counts remaining after one cycle of the program which computes and outputs a new scan and analyzes peak-and-valley count.

3.2.4 Test Results

Table 1 was the result of a test run with the program which operated first to remove X and Y translation and then to reduce scale and skew errors. Pull-in was accomplished in nine cycles.

Table 2 shows the results of a test run on the same imagery with the FDBK61 program which tries to reduce all errors simultaneously. This pulled in in ten cycles and the steps were almost equivalent to those in Figure 1, but note the behavior of the scale and skew errors.

Tables 3 and 4 demonstrate the effect noticed in Table 2. These tests were run on identical images with the two programs as described above. The run in Table 3 pulled in in fourteen cycles. The run in Table 4 pulled in in thirty-three cycles. Note how the translation errors in each are reduced correspondingly through the first six cycles. By now, however, the scale and skew counts had introduced such errors that many more cycles were required to resolve them.

Table 5 was the results of a test identical to that in Table 4 except that the imagery was changed. Here the errors introduced in the scale/skew counts effectively prevented pull-in.

Tables 6, 7 and 8 show the dependence of the correlation system on the direction of the image structure present in the picture. In the test shown by Table 6, the structure was perpendicular to X, and X translation was reduced much faster than Y. In Table 7, the test was run with image rotated 90°. Here, Y translation is reduced faster than X. Table 8 shows the results of a test run with the image rotated 45°. The pull-in here, although requiring more cycles, reduces X and Y translations in even steps.

TABLE 1

	X Trans	Y Trans	X Scale	X Skew	Y Skew	Y Scale
1	25	25	256	0	0	256
2	19	25				
3	12	25				
4	4	21				
5	3	15				
6	3	10				
7	1	4				
8	1	2				
9	0	1	256	0	0	256

TABLE 2

	X Trans	Y Trans	X Scale	X Skew	Y Skew	Y Scale
1	25	25	256	0	0	256
2	19	25	259	-1	1	257
3	11	21	260	-1	1	259
4	3	17	258	-0	1	258
5	2	10	258	0	1	257
6	0	2	258	1	1	255
7	0	0	258	0	1	255
8	0	0	257	0	1	256
9	-0	1	257	0	1	257
10	-0	0	257	0	0	256

TABLE 3

	X Trans	Y Trans	X Scale	X Skew	Y Skew	Y Scale
1	25	25	266	0	0	266
2	21	25				
3	16	25				
4	6	24				
5	2	23				
6	2	19				
7	1	17				
8	1	14				
9	1	10				
10	1	5				
11	1	1				
12	1	0				
13	1	0	256	1	0	257
14	0	0	256	1	0	257

TABLE 4

	X Trans	Y Trans	X Scale	X Skew	Y Skew	Y Scale
1	25	25	266	0	0	266
2	22	25	269	-0	-0	267
3	17	24	272	-1	-0	268
4	10	22	275	-2	-0	268
5	6	20	272	-0	-3	270
6	5	16	269	0	-6	272
7	2	10	267	0	-8	272
8	1	4	265	0	-7	271
9	1	-1	264	1	-5	267
10	2	-1	263	1	-5	267
11	1	-3	262	1	-5	265
12	1	-2	261	1	-4	265
13	0	-2	261	0	-4	263
14	1	-1	260	0	-4	263
15	0	-1	260	1	-3	262
16	0	-1	259	1	-3	261
17	1	-0	258	0	-2	261
18	0	-1	258	0	-2	260
19	-0	-0	257	0	-2	260
20	0	-1	257	1	-2	259
21	0	-1	258	0	-2	259
22	-0	-0	257	0	-2	259
23	-0	0	257	0	-1	258
24	-1	0	258	0	-1	258
25	-0	0	257	0	-1	258
26	-1	-0	257	0	-1	258
27	-0	0	257	1	-1	258
28	-1	0	257	0	-0	258
29	-0	1	257	1	-0	258
30	-0	0	257	1	-0	257
31	-1	0	257	0	-1	257
32	0	0	257	0	-0	257
33	0	0	256	0	-0	258

TABLE 5

	X Trans	Y Trans	X Scale	X Skew	Y Skew	Y Scale
1	25	25	256	0	0	256
2	21	21	254	2	-1	258
3	18	17	253	5	-3	262
4	15	14	253	7	-4	264
5	13	13	254	10	-4	266
6	12	11	254	12	-3	267
7	11	10	255	14	-3	268
8	10	10	256	15	-2	269
9	10	9	258	15	-2	271
10	10	8	260	16	-0	272
11	9	7	261	17	0	273
12	8	7	262	17	1	273
13	9	7	263	18	3	273
14	8	6	264	18	4	274
15	8	7	264	19	4	275
16	7	6	264	19	6	275
17	7	7	264	18	7	277
18	7	6	264	18	8	277
19	6	7	264	18	8	278
20	5	6	263	17	9	278
21	6	5	264	17	8	279
22	5	5	264	17	8	279
23	5	5	264	17	8	279
24	5	5	265	17	8	278
25	5	5	266	17	8	278
26	5	5	266	17	9	277
27	4	5	267	17	8	277
28	4	4	267	17	9	277
29	4	4	268	17	9	277
30	4	4	269	18	10	277
31	4	4	270	18	10	277
32	4	4	271	18	10	277
33	4	4	271	18	11	277
34	4	3	272	17	11	276

TABLE 6

	X Trans	X Trans	X Scale	X Skew	Y Skew	Y Scale
1	25	25	256	0	0	256
2	20	24	256	3	-2	258
3	12	22	255	10	-2	258
4	3	16	257	10	-1	253
5	-0	11	260	5	-5	250
6	-1	8	261	2	-7	250
7	-2	7	259	1	-7	250
8	-2	6	259	0	-6	250
9	-1	5	259	-0	-6	250
10	-1	5	259	-1	-6	251
11	-1	4	258	-1	-5	251
12	-1	3	258	-1	-4	251
13	-1	3	258	-1	-4	251
14	-1	3	258	-0	-3	251
15	-1	3	257	-1	-2	252
16	-1	2	258	-0	-2	252
17	-0	2	257	-0	-1	253
18	-1	2	258	-0	-0	254
19	-1	1	258	-0	0	254
20	-1	1	258	0	0	254
21	-0	1	258	0	1	255
22	-1	1	258	0	1	255
23	-0	1	258	1	1	254
24	-1	1	258	0	2	254
25	-0	1	257	0	2	255

TABLE 7

	X Trans	Y Trans	X Scale	X Skew	Y Skew	Y Scale
1	25	25	256	0	0	256
2	22	17	254	4	-3	258
3	20	6	257	5	-9	258
4	18	-0	262	8	-8	256
5	14	-2	265	10	-7	254
6	10	-1	267	10	-5	255
7	7	-0	267	9	-3	256
8	5	-0	267	9	-2	257
9	4	-1	267	7	-1	258
10	3	-1	265	6	-2	258
11	2	-0	264	6	-1	259
12	2	-0	263	5	-0	258
13	1	-0	262	3	-0	257
14	0	-1	261	3	-0	257
15	1	-1	260	2	0	256
16	1	-1	259	2	0	256
17	0	-1	259	1	-0	256
18	0	0	257	0	0	256
19	0	0	257	0	0	256

TABLE 8

	X Trans	Y Trans	X Scale	X Skew	Y Skew	Y Scale
1	25	25	256	0	0	256
2	20	20	254	1	-2	258
3	17	16	254	4	-5	262
4	15	14	254	7	-5	263
5	13	12	254	9	-5	264
6	11	11	255	10	-5	266
7	10	10	257	10	-5	266
8	9	8	256	10	-4	267
9	8	8	258	10	-3	267
10	6	7	259	10	-3	268
11	5	6	258	9	-3	268
12	5	6	258	9	-2	268
13	4	5	257	8	-1	267
14	2	4	257	8	-1	267
15	2	3	257	7	-1	266
16	2	3	257	6	-1	266
17	2	2	257	6	-0	265
18	1	2	258	5	-1	264
19	1	2	257	5	-1	263
20	0	1	257	4	-0	263
21	0	1	257	4	-0	262
22	0	1	257	3	-0	261
23	0	0	257	2	-1	260

Table 9 shows the results of a preliminary test for pull-in range. X and Y translation errors of greater than 10% were resolved as were scale errors up to 17% and skew errors up to 14%.

TABLE 9

	X Trans	Y Trans	X Scale	X Skew	Y Skew	Y Scale
1	40	-40	240	20	0	280
2	35	-43	243	-1	2	286
3	28	-39	243	-24	4	286
4	22	-32	254	-36	8	292
5	18	-28	251	-36	6	295
6	16	-26	249	-36	1	298
7	16	-26	247	-35	-2	301
8	15	-26	247	-30	-2	300
9	14	-26	248	-29	-3	299
10	13	-26	248	-29	-7	296
11	13	-23	253	-29	-12	291
12	13	-18	247	-31	-13	286
13	14	-17	247	-31	-14	283
14	13	-16	247	-28	-14	280
15	10	-14	250	-27	-9	278
16	6	-10	250	-16	-10	274
17	1	- 5	252	- 6	- 2	
18	1	- 4	254	0	1	261
19	1	- 3	256	0	1	261
20	-1	- 2	256	- 2	1	258
21	0	- 2	258	0	1	256
22	0	0	256	0	2	257
23	0	0	257	0	- 1	255

Section 4

INPUT MATERIAL

4.0 INPUT MATERIAL

The photographs shown in Figure 6 are enlargements of the quarter inch square areas scanned during the simulation tests. These were taken from negatives of the U. S. Government's Arizona Test Range. They are samples of near vertical photography with a scale of approximately 1:20,000.

Each area was duplicated with a negative of a different density, making eight sample areas. These are referred to as position 1 light, position 3 dark, etc.

Photographs A and B of Figure 6 are of a mountainous region. Photograph A, however, has several strong dark bands (roads) running through it, while B has much more random information. Photographs C and D are of flatter terrain, with C containing a road and canal and other regular features, and D being the center area of a cultivated field.

Photograph E shows the area from which the regions above were selected.

Fig. 6a

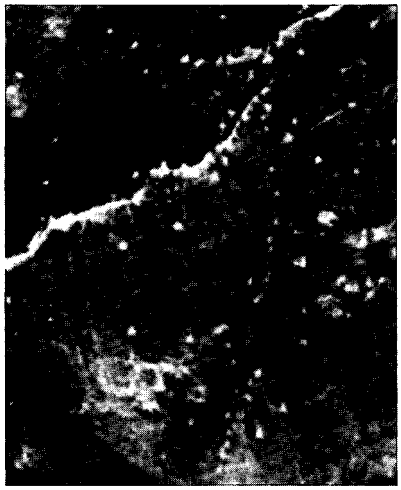

Fig. 6b

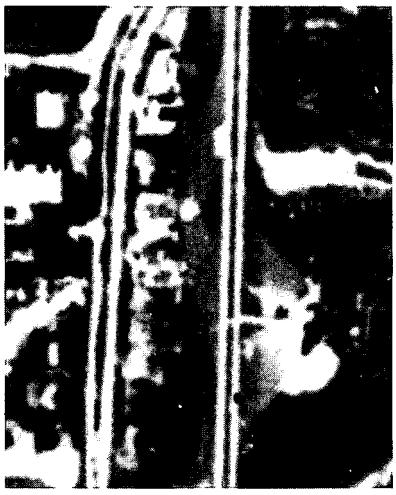

Fig. 6c

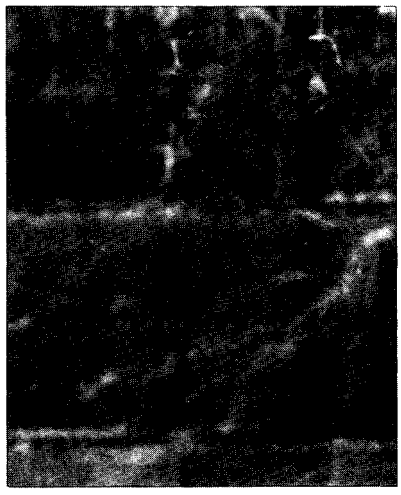

Fig. 6d

Fig. 6e - Images used in parallax detection tests

Section 5.0

TEST RESULTS

5.0 TEST RESULTS

5.1 Inflection Counts

The first series of tests were made to provide information on the range of inflection counts for the different samples of input material. Table 10 shows the variations in inflection counts.

Position Name	Figure 6 Photograph	Inflection Count for Right Scan Raster Size 5 Median	Raster Size 5 Range	Raster Size 4 Median	Raster Size 4 Range
1 light	A	142	138-152	142	134-148
3 light	A	*154	130-176	134	120-148
1 dark	A	124	118-134	130	120-140
3 dark	A	106	96-124	110	98-124
4 light	C	*150	142-162	110	120-136
5 light	C	*154	130-164	122	108-132
4 dark	C	138	130-146	142	134-156
5 dark	C	152	134-184	144	130-164

TABLE 10 SAMPLING REGIONS USED AND THEIR INFLECTION COUNT

In each scan there were 1152 distinct sample points, and so there were at most 1152 possible inflection points. The actual number of inflection points in the right scans, varied from 106 to 154, or from 9.6%to 13.4%. These counts each varied to some degree in repeated scannings on the same sample.

Table 10 shows that the change of raster size made a definite difference in three of the eight positions; 3 light, 4 light, and 5 light (these are marked with asterisks). This variation can be explained in that the areas being repositioned with the raster scale of 4 were not quite those with the scale of 5, and that bands which played a part in the former were not included in the latter. Position 1 light did not have such striking bands; nor did any of the four dark positions.

The left scan was subject to distortions, the distance between successive sample points changing from scan to scan. Therefore, the ratio of spot size to sample distance varied considerably, and the left inflection count did likewise, as shown in Table 11.

Sample Position (Raster Size 5)	Inflection Count for Right Scan Median	Range	Inflection Count for Left Scan Median	Range
4 light	150	146-154	126	120-148
5 light	154	146-158	158	148-166
4 dark	138	136-142	140	132-148
5 dark	152	148-160	160	146-164

TABLE 11 COMPARISON OF RIGHT AND LEFT INFLECTION COUNTS

The difference is especially dramatic in the case of position 4 light, which represents a region where, in conditions of instability, the X scale distortion shrinks to a small value. (See Figures 7 and 8) The range taken in a larger sample is from 98 to 188 and it is generated from tests which include cases where Y scale and Y skew grow 40% and 50%, respectively, to offset an 85% shrinkage of X scale and to give large left scan counts.

5.2 Intensity Settings

Another series of tests was made to determine the optimal intensity setting for each of the eight positions. The left raster was moved towards the right, free of all distortions except X translation, which started at -25 (or 8% non overlap), and moved 5 times (later -35 or 11% and 7 times) to the right with an increment of 5 each time. The X disagreement count would go from as low as -260 to zero, during the 6 (later 8) trials. This test was repeated for different intensities, and the most linear responses in the X disagreement count were recorded in Table 12.

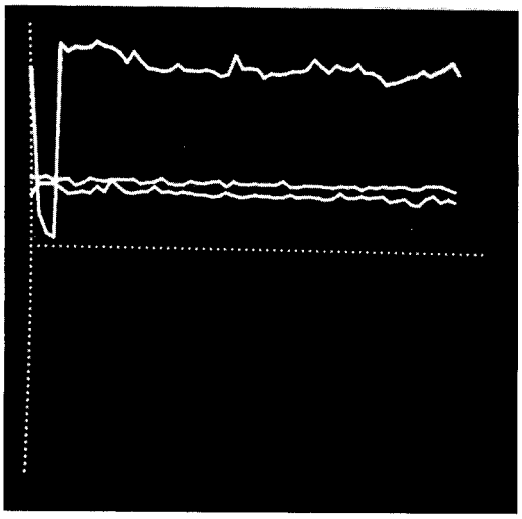

Fig. 7

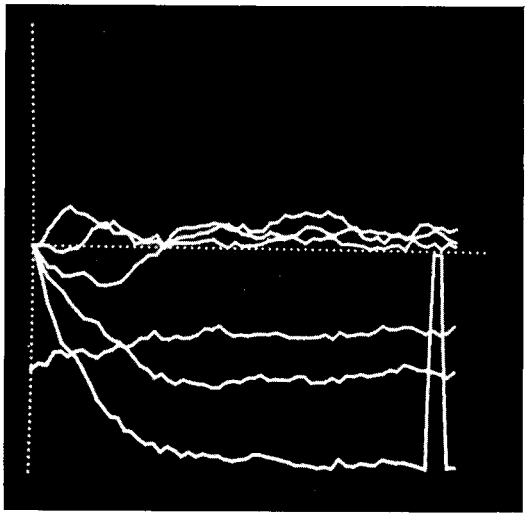

Fig. 8

The above photographs were taken from displays on the large cathode-ray tube shown in Figure 1. Figure 7 illustrates the magnitude of each of the six error signals plotted as a function of cycles through the distortion correction loop. All errors were initially zero except for X translation which started from -70. The constantly decreasing X scale and X skew values prevented pull-in. Scale on the X axis is 1:1; scale on the Y axis 4:1. The sudden discontinuity is caused by overflow of the output buffer and can be ignored.

Figure 8 shows the magnitude of the left and right inflection counts and the total disagreement count as a function of cycles through the distortion correction loop. The X axis scale is again 1:1; but the Y axis scale is 16:1.

Position Name	Best Intensity	Good Intensity
1 light	-107	-100 to -110
3 light	-103	-103 to -107
1 dark	-105	-103 to -115
3 dark	-107	-105 to -115
4 light	-105	-100 to -110
4 dark	-80 (-105)	-75 to -110
5 light	-107	-107 to -113
5 dark	-110	-95 to -115

TABLE 12 X DISAGREEMENT COUNT VS. INTENSITY

The practical limits of intensity were from -120 (very dim spot) to -75 (a bright spot which would remain lit even when in a non scanning state). The median intensity of -105 was chosen. Later, when a raster size of 3 was used for 2 dark, an intensity of -110 was chosen in much the same manner, as -105 was too bright for fine scanning. (This was caused by the changing of the distance between the cathode-ray tube and the photographic plate).

5.3 Total Disagreement Count

For each of the sixteen samplings a series of tests was made to see how great a translation could be introduced and still allow a true lock-on, and another series was made to see how great a distortion could be introduced and still allow a true lock-on. In all cases of lock-on, the number of disagreement counts (left inflection signal disagreeing with right inflection signal) dropped from an initial value between 400 and 700 (34% to 61%) to a set of final values less than 150 (13%). The final values for each sampling were fairly unsteady, but stayed in a range of 50 counts. See Table 13.

Sample Name	Total Disagreement Count Raster Size 5 Median	Raster Size 5 Range	Raster Size 4 Median	Raster Size 4 Range	Pull-In Range Raster Size 5 X_{TR} %		Raster Size 4 X_{TR} %	
1 light	50	35-69	46	35-74	80	25	45	18
3 light	87	70-100	80	70-84	100	31	45	18
1 dark	45	35-64	47	40-84	-75	23	-90	35
3 dark	55	40-64	56	35-69	-110	34	-80	31
4 light	*57	30-79	30	25-39	-52	16	-65	25
5 light	*115	90-124	75	60-84	-100	31	-130	51
4 dark	50	40-64	67	55-89	50	16	60	23
5 dark	128	115-144	112	95-144	120	37	40	16

TABLE 13 TOTAL DISAGREEMENT COUNT

The condition of lock-on is considered here to be met when no distortion varies by more than 6, or 2 1/2% from its true value, and no translation varies by more than 2, or .7% for a raster scale of 5, 1.1% for a raster scale of 4. Each of the counts given in Table 13 stands for only a rough measurement of 9 to 15 trials in the lock-on state.

In almost all cases in which there was not a true lock-on, the various distortions and positions wandered erratically, with one or more of the terms becoming quite large or small. During this wandering, the total disagreement count for each trial was from 300 to 510 with a median at 360 (taken from 35 samples). However, in the trials with a raster size 5 several cases of false lock-on were noted in which the wandering process was halted. Only the cases shown by Figures 9 and 10 had a final range of total distortion which was close to that of the true lock-on, and in both cases, the percentage of distortion for the final trial was quite small. Also the range of distortions for Figure 9 (154 to 132) was far from that of the range for a lock-on condition in the same position (90 to 124), and the range for Figure 10 (80 to 128) was far from that for the range of the lock-on condition for the same position (40 to 64).

Figures 9A and 10A illustrate the behavior of the error signals in cases of false lock-on. In both, all errors are initially zero except for X translation which starts from -110 in 9A and from +60 in 10A. Figures 9B and 10B show the behavior of the inflection counts and the total disagreement count for the false lock-on cases.

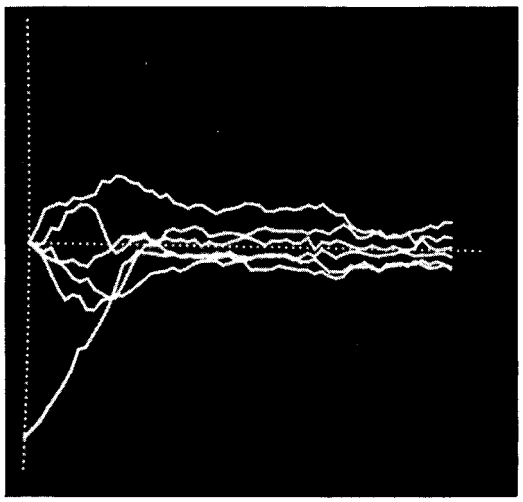

Fig. 9a

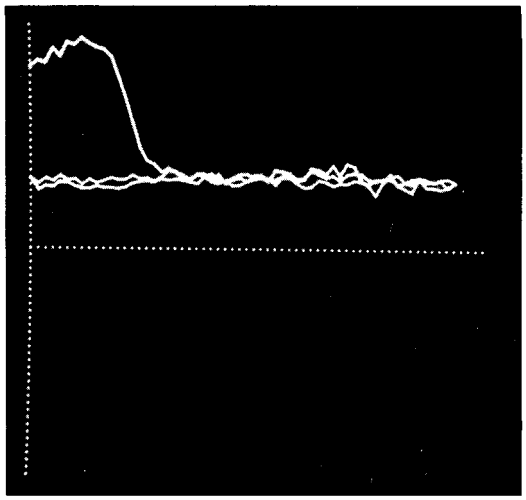

Fig. 9b

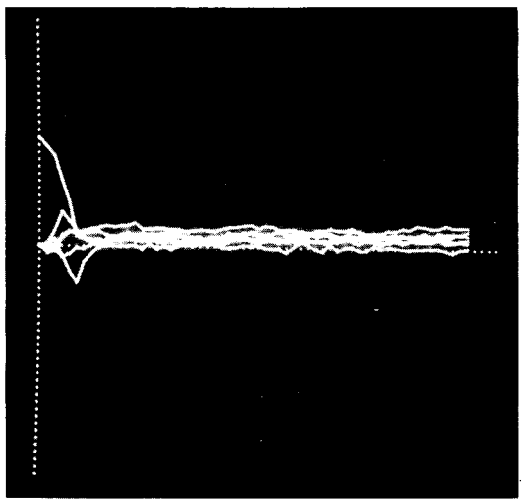

Fig. 10a

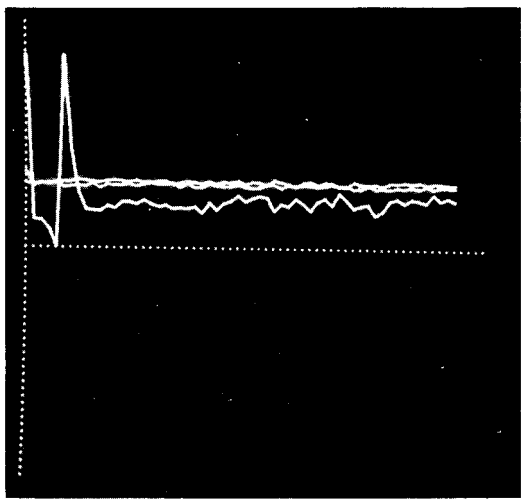

Fig. 10b

Three positions were given close study in order to find the shape of the limits to pulling in for true lock-ons. Two of them with a raster of 4, 1 light and 3 dark, have already been described. The third, 2 dark, is the same general position as 3 dark, but it uses a raster size three fourths the previously mentioned raster, with an optical magnification so that the raster image on the photographic plate was the same size as the image from the previous raster. The resulting area was not quite the same, and the right scan inflection counts were smaller, so that the region has been considered to have new imagery and has been called position 2 dark. (The intensity of the scanning spot also had to be reduced to -110).

5.4 Pull-In Range

The major portion of the test program was devoted to determining the pull-in range capability of the system. This was done first for each of the six error items independently, and then for different combinations.

Pull-in range is described both in terms of the distance between the center points of the right and left scans and, for those cases in which the left scan is undistorted, in terms of the percentage of area of the right scan raster which is not overlapped by the area of the left scan raster. The range is found by moving the left raster out from the right raster such that the line between their center points has a constant slope angle. For each slope angle tested, there is a distance beyond which there is not a true lock-on, and inside of which there is a true lock-on.

The pull-in distances are given in Table 14.

Angle	Distance	Percent Non-overlap	Number of Trials Lock-on	Decrease Count	Cause for Pull-in	Major Disturbing Factor	Minor Disturbing Factor
POSITION: 1 light							
0°	50	19	12	12	Xtr	Ysc	Xsk
30°	50	24	25	28	Xtr	Xsc	Ysc,Xsk
60°	55	25	20	18	Ytr	Ysk	Ysc,Xsk
90°	55	19	30	30	Xtr	Ysk	Ysc,Xtr
120°	54*	25	16	15	Ytr	Xtr	
POSITION: 3 dark							
0°	62*	24	55	56	-	Ysc	Xsc
30°	52	25	63	63	-	Xt	Xsc,Ysc
45°	86	40	126	126	Ytr	Ysc	Xsk
60°	102*	45	101	101	Xtr	Ysc	Xsk
90°	96*	33	63	58	Ytr	Ysc	Xsc,Xsk
135°	125*	38	60	60	Xtr	Ysk	
150°	108	37	42	44	Ytr	Xsk	Ysk,Ysc
180°	64	25	32	33	Xtr	Ysk	Xsc,Ysc
210°	80	37	29	28	Xtr	Xsc	
225°	77	38	29	26	Ytr	Xsc	Ysk
270°	64	22	26	26	Ytr	Xsc	Ysc,Ysk
300°	88	41	20	24	Ytr	Xsc	Ysk
330°	138	59	24	33	Xtr,Ytr	Xsk	
POSITION: 2 dark							
0°	104*	55	108 (103)	99	Xsk	Xsc	Ysk
45°	97	67	63+		Xtr	Xsc,Ysc	
90°	111	49	47	48	Ysc	Xsk	Ysc
135°	84	50	34	40 (32)	Xtr	Ysk	Xsk
180°	134*	70	57	54	Xtr	Xsk	Ysk,Ytr
225°	94	54	63+	-	Xtr	Ytr	Xsc,Ysc
270°	137	64	63	63	Xtr	Ysc	Xsc
315°	77	46	41 (55)	54	Ytr	Ysk	Xsc,Ysc

TABLE 14 PULL-IN RANGES AND RELATED VARIABLES

AS A FUNCTION OF SLOPE ANGLE

!?

It can be seen that the pull-in range can vary with the angle of translation, as it did for position 3 dark (a distance of from 52 to 138, or 24% to 59% non-overlap of rasters) and for position 2 dark (84 to 134 or 49% to 70%), or, that it can remain relatively constant, as it did for position 1 light (50 to 54 or 19% to 25%). The minimum range in Table 14 was 19%, and in Table 13 figures on other sampling areas show that for a set of tests taken in one direction (either 0° or 180°) the minimum range decreases to 16%. It is somewhat harder to measure the median range because several of the pull-in trials were ended by CRT overlap, a condition in which the left scanning raster moves so far in one direction that it goes off the edge of the tube and returns on the opposite side. This usually causes one of the distortions to grow indefinitely, and there was no way of determining if such a growth would have occurred if the overlap were absent. These cases are marked by asterisks in Table 14.

If, however, these values are lumped together, the median was about 40% (35% if the ranges ended by overlap are dropped from consideration). The maximum pull-in was 67%.

The number of trials required for pulling in from an initial distortion and/or translation to a true lock-on varied roughly with the distance to be pulled in from, but only very roughly, as can be seen by comparing columns 2 and 4 (or 3 and 4) of Table 14. The ratio of number of trials to radial distance between center points for position 3 dark alone varied from .6 to 5.7.

The total disagreement curve, as in Figure 11, came in to a minimum value at about the same place where the two translation and four distortion curves came together in Figure 12. This relationship can be seen to hold generally by comparing columns 4 and 5 in Table 14. In those places where the two minimums are different, there is a secondary minimum in the total disagreement curve, or another place in the set of distortion curves where the six curves come near zero.

When lock-on fails to occur, this is usually the result of an aberation growing in the scale and skew distortions, rather than an aberation in translational position. Column 7 of Table 14 shows the particular variation which seems to expand most sharply and to grow uncontrollable most rapidly in the first few trials. In 15 cases, it is a scale variable, 9 cases a skew variable and in only 3 cases is it a translation variable. Table 15A gives a condensation of this data.

Figure 11 illustrates the behavior of the inflection counts and total disagreement count for a lock-on case. The disagreement count went from 608 to 48. The sudden discontinuity is due to overflow of the output buffer.

Figure 12 illustrates the interacting behavior of the six error signals. Both X and Y scales initially enlarged to try to compensate for the introduced translation error. All errors (except for X translation) reached their peaks at about the same time, but were pulled in at different rates.

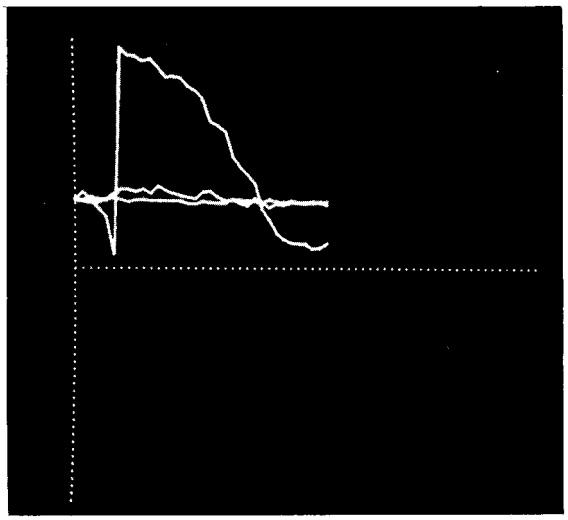

Fig. 11

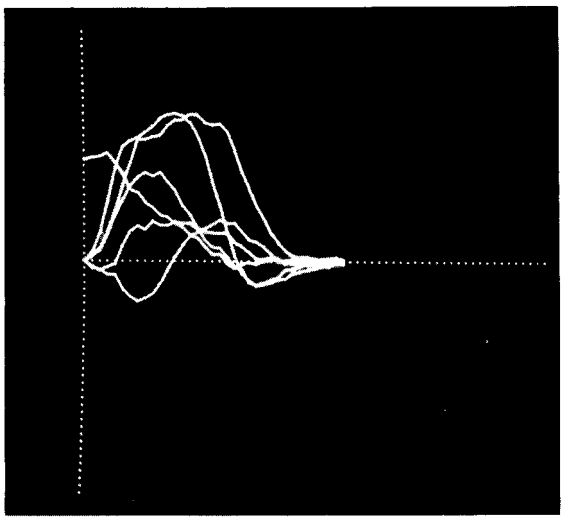

Fig. 12

Xtr	Ytr	Xsc	Xsk	Ysk	Ysc		Xtr	Ytr	Xsc	Xsk	Ysk	Ysc
		4	1	2	6				8	5	4	12
		4	2	4	1				7	6	8	6
2	1	8	3	6	7	Totals	3	2	15	11	12	18
		A							B			

TABLE 15 NUMBER OF PRINCIPLE AND CONTRIBUTING ABERATIONS AMONG 26 CASES

It is hard to be sure if the most active aberation was the one which actually was most responsible for there being no true lock-on and in some cases, there were several other aberations going on at a lesser rate. Column 8 of Table 14 shows these aberations, and Table 15B presents a condensation of Columns 7 and 8 together. Again, it can be seen that translation tended not to be an aberation as often as scale or skew did, but there is still a question as to whether or not scale occurs as an aberation significantly more than skew.

It is further worth noting, that of the fourteen directions considered for position 3 dark, eleven of them occur with one or the other of the translations moving initially so as to decrease the disagreement between left and right scan. This tentatively implies that we would have better results from a test procedure which would act on translation first.

When lock-on occurs, it appears as if variables with initial aberations are being caught and compensated for by other variables which move the state of the left scan into such a condition that it is able to decrease disagreement. The most active corrective variable is probably the one which moves toward zero disagreement the fastest, and Column 6 shows that for the test in extending translation this corrective variable was a translation variable.

Tests were performed to see what the effects of initial distortion would be. These tests were first done with only a single variable. Then the pull-in range was tested for initial displacement along slope angles to see how the distortions might modify the general contours.

Due to overlap considerations X scale was diminished instead of expanded until there was no lock-on. When overlap in translational testing necessitated changing raster size by four fifths, the X scale test was repeated and an X skew test performed. The results are given in Table 16. Skew figures are to the nearest 6% and scale figures to the nearest 3%.

Position	X Scale Percent Diminished (Raster Size 5)	X Scale Percent Diminished (Raster Size 4)	X Skew Percent Diminished (Raster Size 4)
1 light	81	66	89
3 light	31	97	89
1 dark	66	75	50
3 dark	97	97	100
4 light	47	97	89
5 light	91	75	100
4 dark	97	81	100
5 dark	84	69	50

TABLE 16 PULL-IN RANGE FOR SCALE AND SKEW

For the skew figures, the percentage is based upon the fact that if a square raster under 100% distortion were superimposed upon itself with center point touching center point, the upper edge would be moved over so far in one direction that its midpoint would coincide with the corner of the undistorted square, and the lower edge would move equally far in the opposite direction.

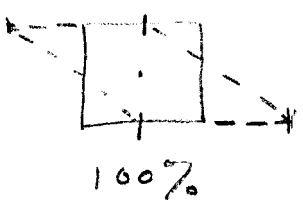

One hundred percent X scale diminishment means that the left raster becomes a vertical straight line, if the other distortion variables have their normal values. So, 97% diminished distortion in X scale is an extreme case indeed; it is equivalent to an expanding scale distortion of 3200%. The minimum X scale distortion is 31%, the median is 81%, and the maximum is actually over 150%, for at position 3 dark, raster size 4, a test was made with an initial X scale distortion of -1/2, starting from a mirror image. (The opposite sort of behavior occurred for position 4 dark, raster size 4, in that initial X scale distortions of 88% or more went to negative values.)

The minimum X skew distortion was 50% with a median of at least 89%. However, overlapping of the raster on the cathode-ray tube occurred for half the tests, so that a smaller raster might have allowed a much greater skew range.

5.5 Edge Effects

The presence of distortions modifies the translational pull-in range for a slope angle, but it does not necessarily decrease it, as is shown in Figure 13.

The X scale distortion expands the range in only one out of the fourteen cases, but the Y scale distortion expands the range in five out of thirteen cases.

The minimum pull-in range drops to 12% for X scale diminished by 25%, the median is 31%; and the maximum over 63%, although it is only 39% for position 3 dark. The minimum pull-in range for Y scale diminished 25% is 16%; the median is 37%; and the maximum is over 63%, and 55% for position 3 dark. Thus, the median is slightly increased over our value of 35% for the condition of no initial distortion. (Slope angles for which the pull-in range is determined by cathode-ray tube overlap are marked by bars on top of them in Figure 13. They are left out of the immediately preceding calculations).

The percent of non-overlap of the right scan is actually somewhat larger than calculated above, as the left raster is smaller due to the scan distortion. However, there is the problem as to which should be considered, the percentage of the area of the right scan left uncovered, or the percentage of the area of the left scan remaining uncovered. These two assumptions give radically different answers, and so, as a compromise, it has been assumed that the left scan is the same size as the right scan, neither larger nor smaller. This case makes the change in percentage of non-overlap due to distortion have roughly the same proportion as the change in radial distance.

Examinations to see if the effects of a scale distortion on pull-in range could be accounted for in terms of the aberations were conducted. For example, a diminishing of X scale might improve the pull-in range if one of the major aberations is an expanding X scale factor, in that the translation variables would be able to come in while X scale would be expanding back to and through normal values. It was determined that there is probably no direct explanation for the changed pull-in range of a distortion being found either in terms of the initial scale distortion or in terms of the behavior under a scale distortion forced later by some other variable to become very large or very small.

5.6 Image Change

Figure 13 shows a direction, 30°, for which the pull-in range without distortion is represented by two values. The closer value always pulls in, while beyond the further, Y scale blows up to a large value and overlap, and X scale becomes small. In between these two values the behavior was variable. One day, X scale would expand 25%, and crawl in an aimless fashion, never locking on. Another day, it would expand only 15%, and crawl in to an eventual true lock-on.

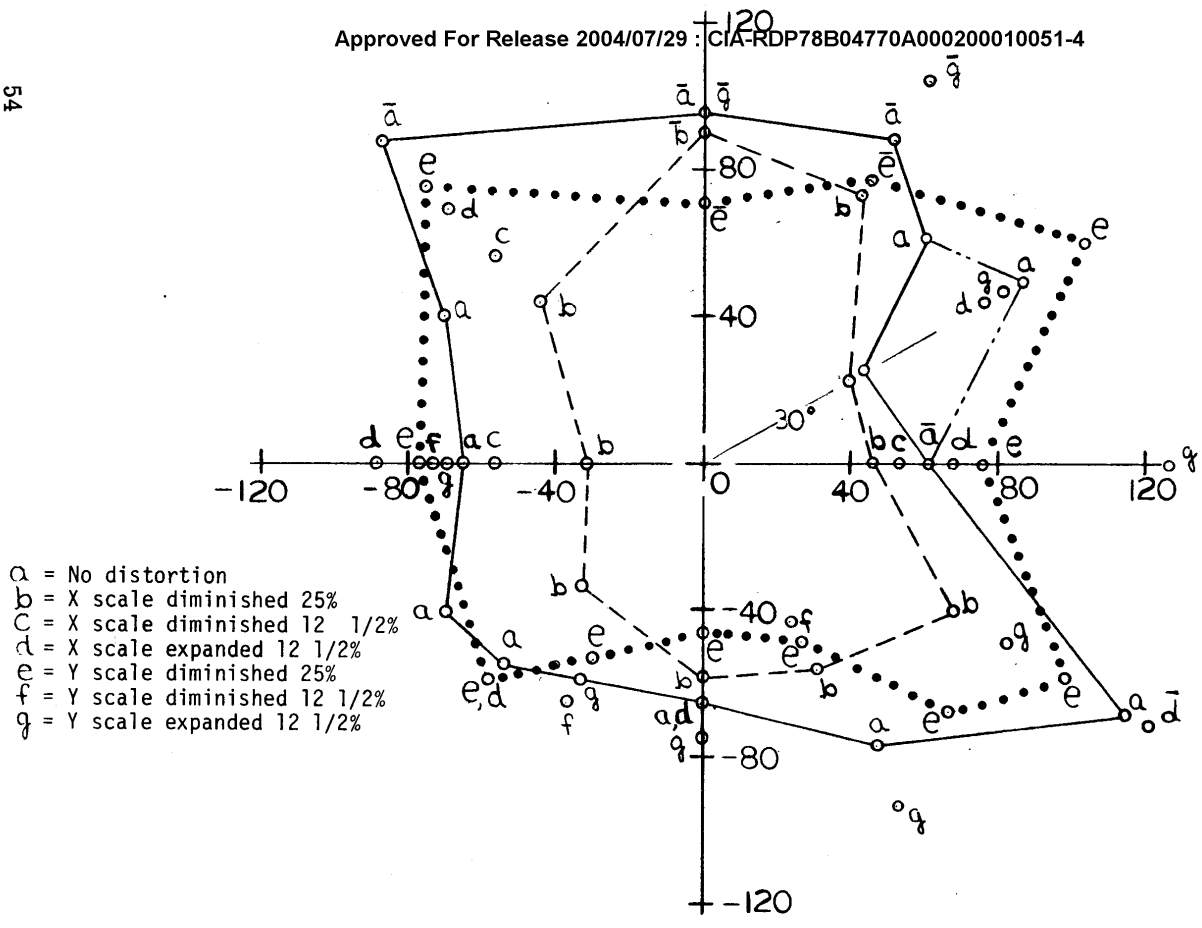

FIG-13

PULL-IN RANGE FOR POSITION 3 DARK AS MODIFIED BY SCALE DISTORTIONS

This change in behavior did not seem to occur for 180° or 270°, perhaps because they both tended to have strongly aberating variables beyond the pull-in range instead of aimlessly wandering variables. A change in behavior was observed with slope angle 0° for position 2 dark, where at first, Y skew was growing to a distortion of almost 100%. Later, a check of spot size and intensity showed that constant values had wandered from their settings, and when they were replaced, the skew distortion was reduced and the pull-in range was extended from 62 to 104. Later, in measurements at 90° and 45°, a sharp rise of Y skew distortion could be used to indicate a slight change in these constant values.

Tests were made at position 3 dark to see if smaller initial distortions would affect the pull-in range in the same way. The results were scattered. In general, X scale was regular in its behavior, in that an initial diminishing of 12% extended the pull-in range (marked as "c" in Figure 13), and an initial expansion of 12% extended it still more, (marked as "d" in Figure 13), although not necessarily beyond the undistorted range. The results for Y scale were not so orderly, as is shown in Table 17. (The dot between items means that the item on the right is only slightly larger than the item on the left). Of the 9 cases, g (12% expansion) was clearly greater than e (25% contraction) six times, less than it twice, and roughly the same once. The values of f (12% contraction) were close to those for e, but slightly bigger twice, and slightly smaller twice.

Slope Angle	Order of Pull-In
0	$\bar{a}$ e g
30	a g . e
60	$\bar{e}$ $\bar{a}$. $\bar{g}$
90	e a g
180	a . g . f . e
240	e g . f
270	e . f a g
300	f . e a g
330	g e a

TABLE 17 PULL-IN RANGE AS AFFECTED BY INCREASING INITIAL DISTORTION IN Y SCALE

Another series of tests were made to determine pull-in behavior in the presence of an initial X skew distortion of 64 or 25%. The results are given in Table 18.

Position 1 light

Angle	Distance	Percent Non-Overlap	Change in Distance (with respect to undistorted case)	Change in Percent
0	21	8	-29	-1-
30	20	10	-30	-14
60	31	15	-14	-10
90	46	16	- 9	- 3
120	44	21	- 2	- 4

Position 2 dark

Angle	Distance	Percent Non-Overlap	Change in Distance (with respect to undistorted case)	Change in Percent
0	70	36	-34	-19
45	67	40	-30	-17
90	94	43	-27	- 6
135	100	58	+16	+ 8
180	140	73	+ 6	+ 3
225	67	40	-24	-14
270	77	36	-60	-28
315	62	38	-15	- 8

TABLE 18 PULL-IN RANGE AS AFFECTED BY A 25%

X SKEW INITIAL DISTORTION

The pull-in range, as with X scale, was generally decreased with a median of 10%, a maximum of 28%, and a maximum increase of 8%.

The presence or absence, in the corresponding undistorted test, of either an initial X skew aberation or an increasing aberation did not consistantly improve or worsen the pull-in range. The initial behavior was also mixed, in that X skew definitely worsened five times, improved three times, stayed constant three times and twice changed its behavior from getting worse outside the pull-in limit to getting better inside the limit.

5.7 Inflection Count As A Feedback Factor

Tests were made in which the changes in distortion and translation, which were derived from the disagreement counts, could be modified by the average of the right and left scan inflection counts. The results for position 3 dark were inconclusive, as the usual inflection count value (120) was about the same as the constant in the unmodified case (128), and so it was not surprising when the pull-in ranges for slope angles 180° and 270° were the same as they had been before. The results for position 2 dark showed an extension from 97 to 101 for slope angle 45°, (about 4%) and from 84 to 88 for slope angle 135°, with inflection counts around 93. Figures 14 and 15 for the former case look similar, but the presence of modification from inflection count has the effect of making the distortion changes more abrupt. Figures 16 and 17 are somewhat more dissimilar, but the aberant variables behave in much the same way beyond the pull-in region. The modification did not seem to make significant difference.

Figures 14 and 15 compare the behavior of the correlation system with and without normalization by inflection count. The behavior was almost identical, and both cases finally ended in a lock-on state. In 14A the initial errors were X and Y translations of 72; in 15A they were X and Y translations of 69.

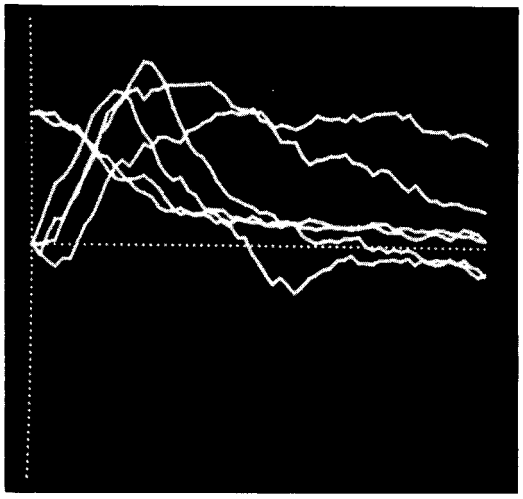

Fig. 14a

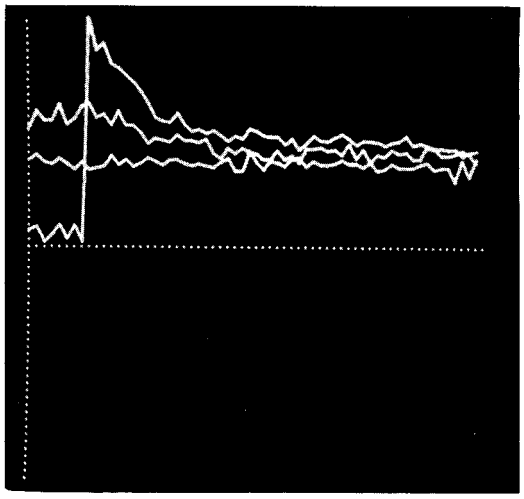

Fig. 14b

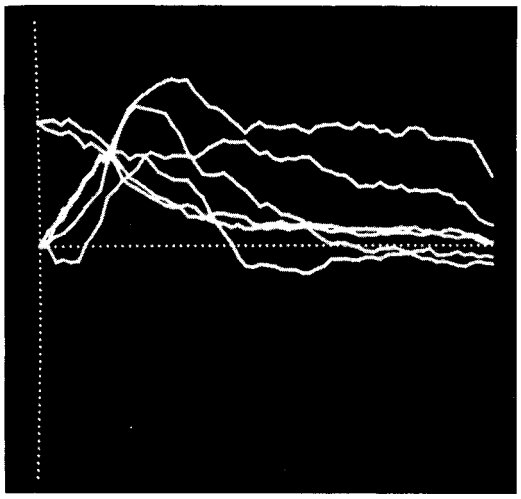

Fig. 15a

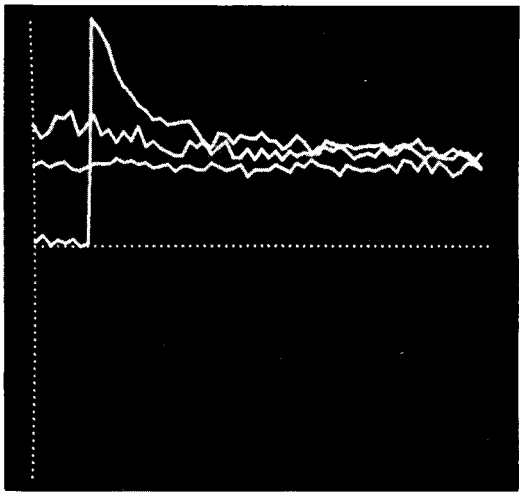

Fig. 15b

Figures 16 and 17, like Figures 14 and 15, compare the behavior of the correlation system with and without normalization by inflection count. Again the behaviors are similar, and the pull-in ranges, 63 and -63, for the normalized condition vs. 59 and -59 for the non-normalized one, are almost the same. It is the X scale variable which expands so much in both cases.

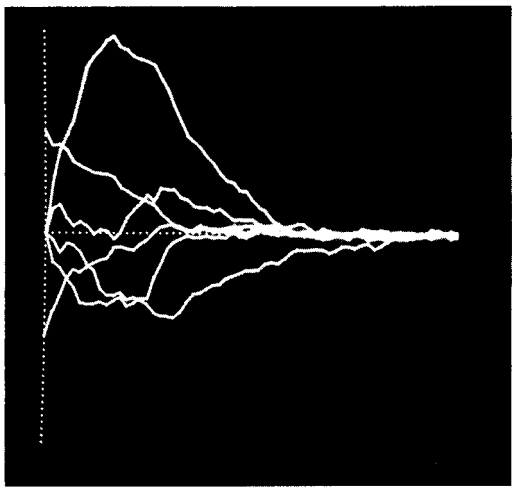

Fig. 16a

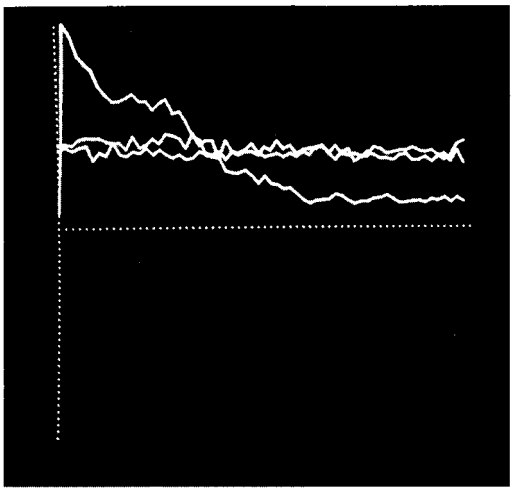

Fig. 16b

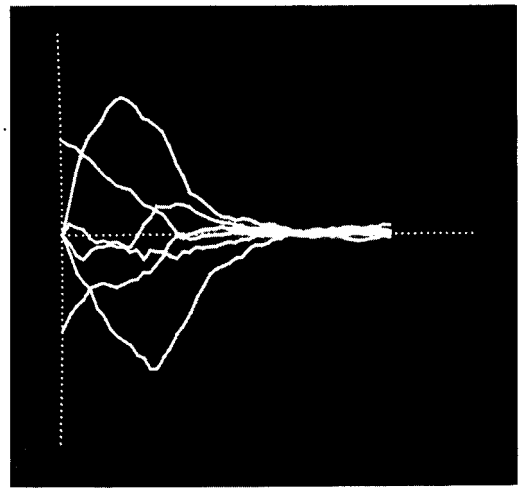

Fig. 17a

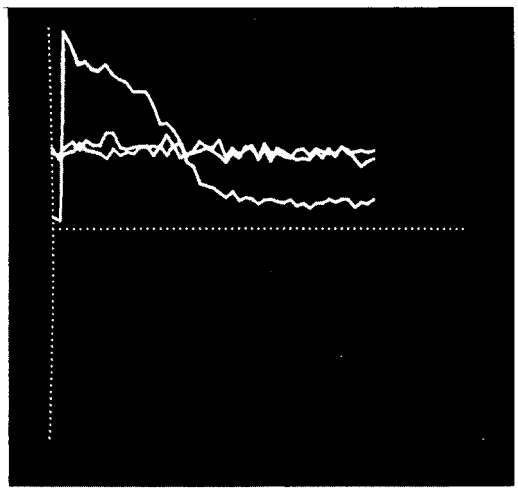

Fig. 17b

5.8 Spot Size

It has been mentioned that a change in effective spot size was responsible for the wide ranges of values for the inflection count of the left scan. Change in spot size was investigated by testing several slope angles of position 3 dark for pull-in range with spots that were bigger (5.5 sample points to cross a spot diameter), and smaller (3.5 sample points to cross a spot diameter). The previous samples had taken 4.5 sample points to cross a spot diameter which was thus of length equal to 3.5 times the distance between sample points.

It was expected that the use of a larger spot would decrease the number of inflection points, in that intensity changes would be summed over a larger area, with the result that rapid changes of intensity would be averaged, and show up in the output only as fluctuations in intensity too small to change the state of the inflection detector circuit. Thus, only changes in general intensity levels which occur over a large area would cause large enough intensity fluctuations to change the state of the inflection detector circuit, and so the inflection count would go down. Use of a smaller spot would allow smaller fluctuations to change the state of the inflection detector circuit, and the inflection count would be raised. Columns 2 and 3 of Table 19 shows that this relationship does hold.

	Right Inflection Count		Pull-In Range Distance		Percent	
Spot Size	Median	Range	Median	Range	Median	Range
2.5	144	134-154	51	40-78	23	17-35
3.5	124	110-134	80	62-125	33	22-41
4.5	104	96-114	90	60-122	38	21-53

TABLE 19 PULL-IN RANGE OF AFFECTED BY SPOT SIZE

It was also noted that the increased spot size generally improves the pull-in range, although not always, as Figure 18 shows.

Figure 18 also indicates that the contour of the pull-in range varies sharply as the spot size varies.

This may be accounted for, in that an increase in spot size rules out many of the intensity changes which are of a high spacial frequency, and so the photographic image scanned is different imagery. So, the data in Table 18 is of more statistical value than structual value.

5.9 Position Change

A small change in position can also change imagery and the pull-in range. Position 2 dark was taken, and the right scan center point was raised at the image holder 5 times by increments of 6 units each time. After each raise, the left scan was extended at a slope angle of 315° to see how the pull-in range would be affected. The percentage held at around 46.9 for three positions, rose to around 63% for the next two trials, and then rose up to 76% for the last position. The values are shown graphically in Figure 19. Thus the distance almost doubles to 148, and the percentage of non-overlap goes up to 30%, with a distance change of 30, or 14% of the raster height.

Figures 18 and 19 also show a variation in contour for the pull-in range. Position 3 dark seems to have a rectangular shape, save for the values shooting out around 135° and 315°. However, the same position under a larger spot size has a more square appearance, and under a smaller spot it develops a diamond shape (save for 315°) very much like that of position 2 dark.

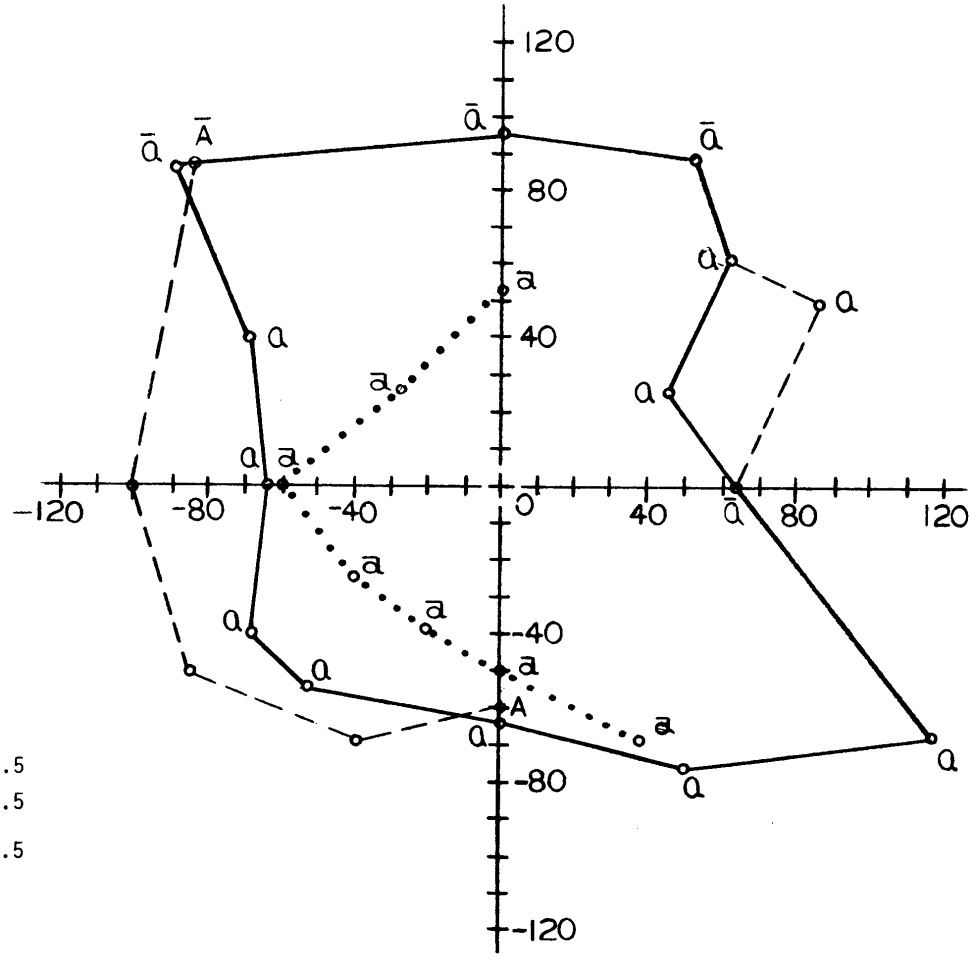

a = Spot Size 3.5
A = Spot Size 4.5
a = Spot Size 2.5

FIG-18

PULL-IN RANGE AS AFFECTED BY SPOT SIZE

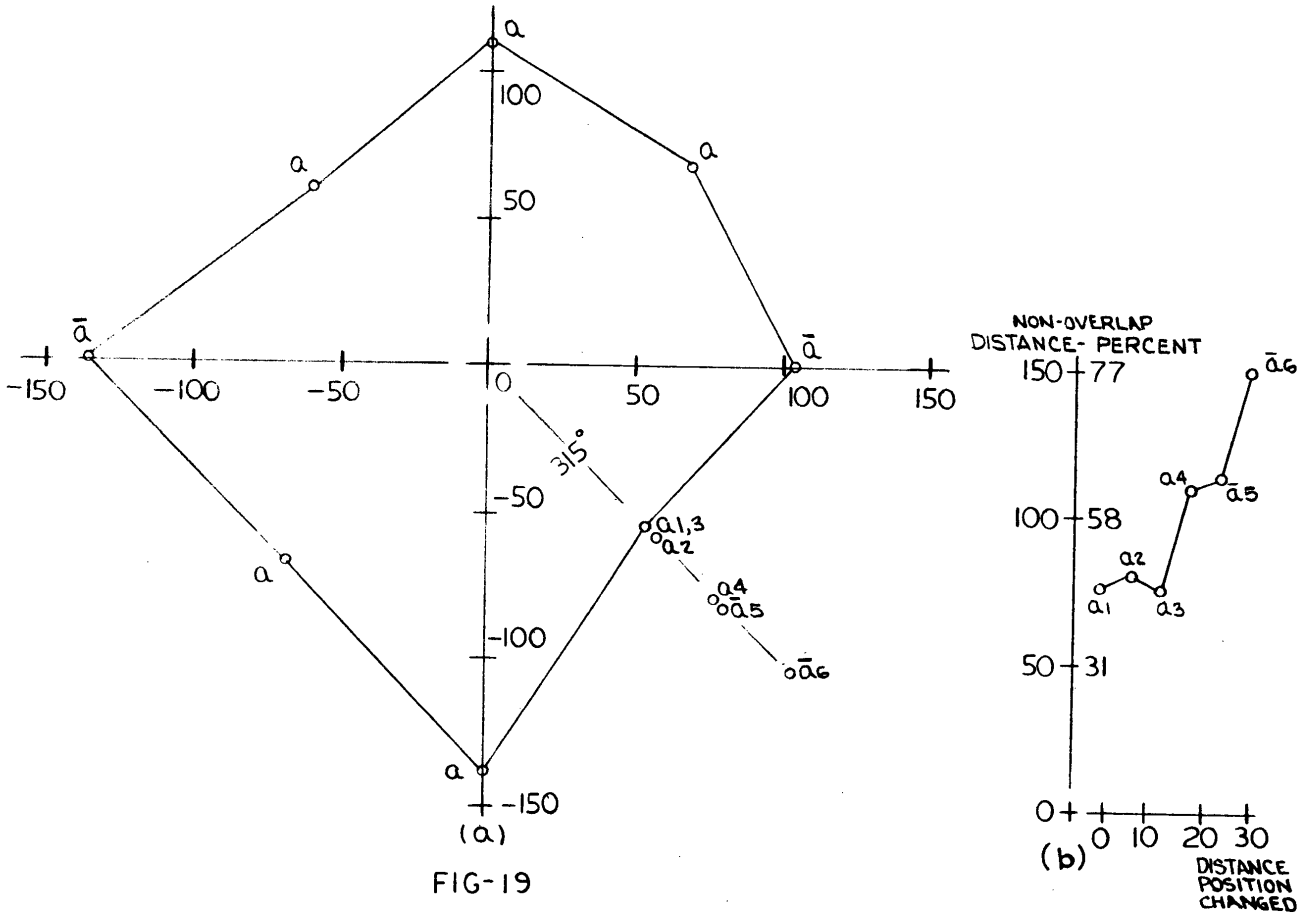

FIG-19

PULL-IN CONTOUR FOR POSITION 2 DARK AND PULL-IN RANGE AS AFFECTED BY SMALL POSITION CHANGE

5.10 Extreme Case

Figure 20 illustrates an extreme case in which pull-in was accomplished. The corresponding initial rasters are shown in Figure 21. Translation errors of 42%, scale errors of 75% and 63%, and skew errors of 38% and 12% are reduced simultaneously to lock-on values of less than 2%.

It is obvious that this case is far beyond what can reasonably be expected of the correlation system, however, the errors were introduced systematically and pull-in was accomplished for all cases leading up to the limits mentioned above, and for no cases in which these limits were exceeded. The explanation must be found in terms of the image content.

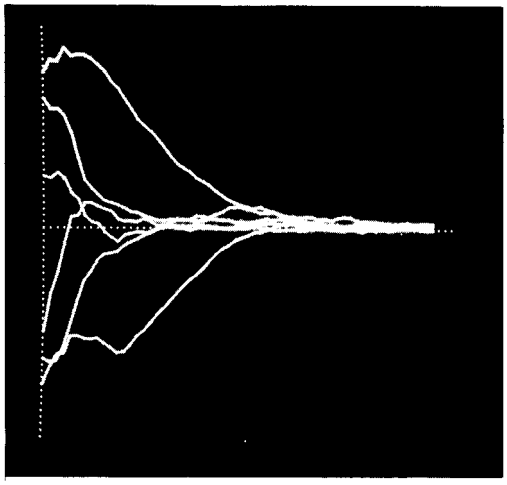

Fig. 20

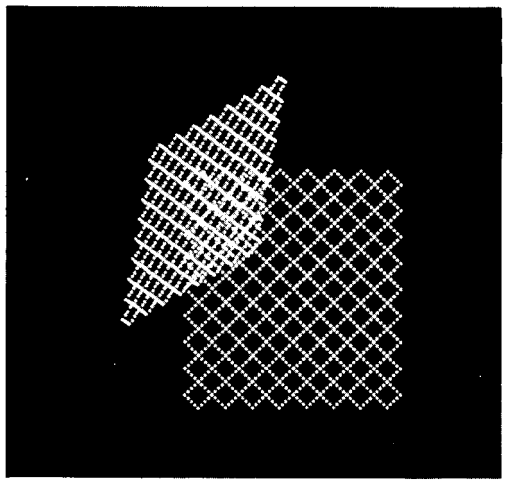

Fig. 21

Section 6

CONCLUSIONS

6.0 CONCLUSIONS

Based on the preliminary results in Section 3 and the final results of Section 5, the following list of conclusions appears to be well justified:

A. The pull-in range and number of trials required to clear distortion vary greatly depending upon image content. The translation range extends from 16% of non-overlap of area to 67%, and for any one position may vary 30% for different directions from the center point. The scale range extends from a minimum of 31% to a maximum of 97% with a median at 81%. The skew range has a minimum of 50%, a maximum of over 100%, and a median of 89%. The number of trials necessary for pull-in varied from 5 to 140, and was dependent on amount of translation and distortion introduced and on image content.

While these results were, admittedly, beyond the expected abilities of the simulation system, it is felt that they do not exceed the theoretical limitations. (See Section 1.1) (Inconclusive)

B. The inflection count varies greatly for different regions and even varies slightly for repeated scans of the same region. It was determined that no significant improvement is realized if this count is used as a normalizing factor in distortion correction.

C. The optimum intensity varies for different regions of the photograph, and greatly affects pull-in capabilities. Therefore, any such system should have an intensity monitor and automatic intensity control.

D. The disagreement count is reduced in all lock-on cases, but the final value varies with image content. This final value is less for true lock-on cases than it is for false lock-on cases, and sensor circuitry could detect the difference.

E. The total disagreement curve comes to a minimum on about the same trial as the minimum error occurs between the six left scan distortions and translations. This minimum could be used to signal "lock-on".

F. Pull-in range is generally decreased as the scanning spot size decreases, and increases slightly with small increases in spot size.

G. In most cases the variable which most assists lock-on is a translation variable, and a system removing translation errors before acting on the other distortions would provide greater pull-in range and stability.

H. Any one of the six variables may be the most disruptive variable (that which acts so as to prevent lock-on).

I. The presence of a particular distortion may actually serve to extend the pull-in range, but no definite relationships could be determined.

#4176

1. SIMULATION.

a. Reduce transit initially?
b. -% is high (19-67% Translation) for pull-in!!

- Scale: 31-97%
- Skew: 80-100%

WHAT'S WRONG?

A. The "theretical" limitations proven by this test appear to lack useful relation with A.SS. expected. The percentages are far higher than expected

B. Are they considering the disagreement count to differentiate between true and false lock-on? Doubt it. Should they?

C. Need more study of spot size effect - how apply to actual ASS? Does HPSC use finer spot for greater lock-on precision?, at sacrifice of Pull-in range?

★ D. Useful fact applied to ASS is sequential actions on translation, scale, skew distortions.

How use H and I. (p. 70) in future?

APPENDIX I

The deflection distortion system seeks to apply zero and first order distortions between the scans on the 2 image dissectors such that conjugate points will be scanned at the same time.

If an undistorted scan produces deflections x (t) and y (t), the distorted deflections on the two tubes may be expressed as:

$$x_1 = x + \frac{\Delta x}{2}$$

$$y_1 = y + \frac{\Delta y}{2}$$

$$x_2 = x - \frac{\Delta x}{2}$$

$$y_2 = y - \frac{\Delta y}{2}$$

where,

$$\Delta x = a + bx + cy$$
$$\Delta y = d + ex + fy$$

The six components of the distortion signal are:

a x parallax

b x in x

c y in x

d y parallax

e x in y

f y in y

It is desired to extract these 6 components from the disagreement detection outputs with an undistorted scan, such that the scan may be dynamically corrected.

Let us examine how the peak and valley detector observes a portion of the picture near a peak (intensity maximum) in the image. Let x_1, y_1 be the location of a peak on

Figure 1

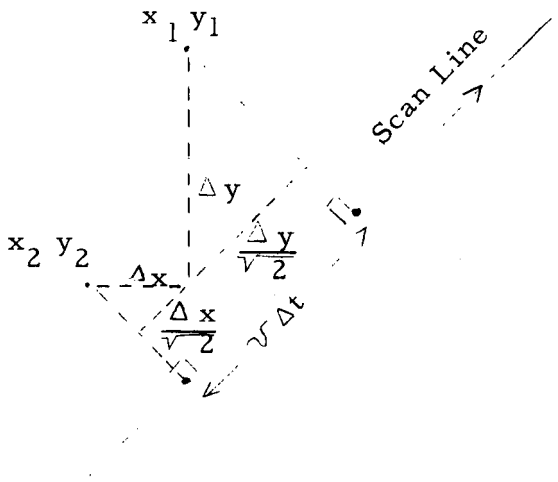

Image 1 and x_2, y_2 by the location of the conjugate peak on image 2. The scan is undistorted so a single scan line is shown on the figure.
Assume the peak is seen by each pv detector when the scan on the respective image tube passes closest to its location in the image. It may be seen from the figure that the distance along the scan line between the conjugate peaks is

$$\frac{\Delta x}{\sqrt{2}} + \frac{\Delta y}{\sqrt{2}}$$

The disagreement time is therefore, $\Delta t = \frac{\Delta x + \Delta y}{\sqrt{2}\, v}$ where v is the scanning spot velocity. The disagreement is initiated in image 2 so the disagreement signal will appear on the line labeled "2 unit" on the block diagram.

The scan line can go in four different directions, depending on the values of $\dot{\underline{x}}$, $\dot{\underline{y}}$ where $\dot{\underline{x}}$, $\dot{\underline{y}}$ take on the values ± 1. The figure shows the case of positive $\dot{\underline{x}}$ and $\dot{\underline{y}}$. The scan direction will affect the sign of the terms in the disagreement so that for any direction of scan passing near a peak or valley, the disagreement contribution

$$\mathcal{E} = 2 \text{ init} - 1 \text{ init} = \frac{1}{\sqrt{2}\, U} (\dot{\underline{x}}\, \Delta x + \dot{\underline{y}}\, \Delta y)$$

In the following, it will be assumed that the number of disagreements seen during one frame scan is large and that the disagreements are uniformly distributed with respect to the scan variables x, y, $\dot{\underline{x}}$, $\dot{\underline{y}}$, so that for instance, the number of disagreements seen with $\dot{\underline{x}}$ positive is about the same as the number seen with $\dot{\underline{x}}$ negative.

In the block diagram the first cross switch effectively creates the function $\dot{\underline{x}}$ as the difference between the two output lines. The integrator effectively sums up all the disagreements in the frame.

Expanding our expression for a single disagreement:

$$\mathcal{E}_\lambda = \frac{1}{2} (a\, \dot{\underline{x}} + b\, x\, \dot{\underline{x}} + c\, y\, \dot{\underline{x}} + d\, \dot{\underline{y}} + e\, x\, \dot{\underline{y}} + f\, y\, \dot{\underline{y}})$$

multiplying by $\dot{\underline{x}}$

$$\dot{\underline{x}}\, \mathcal{E}_\lambda = \frac{1}{\sqrt{2}\, U} (a + b\, x + c\, y + d\, \dot{\underline{y}}\, \dot{\underline{x}} + e\, x\, \dot{\underline{y}}\, \dot{\underline{x}} + f\, y\, \dot{\underline{y}}\, \dot{\underline{x}})$$

Note that $\dot{\underline{x}}^2 \equiv 1$ so $\dot{\underline{x}}$ disappears from the first three terms.

Summing over the frame scan

$$\sum_{\lambda=1}^{n} \dot{\underline{x}}\, \mathcal{E}_\lambda = \frac{n}{\sqrt{2}} \left(a + \frac{b}{n} \sum_{\lambda=1}^{n} x + \frac{c}{n} \sum_{\lambda=1}^{n} y + \frac{d}{n} \sum_{\lambda=1}^{n} \dot{\underline{y}}\, \dot{\underline{x}} + \frac{e}{n} \sum_{\lambda=1}^{n} x\, \dot{\underline{y}}\, \dot{\underline{x}} + \frac{f}{n} \sum_{\lambda=1}^{n} y\, \dot{\underline{y}}\, \dot{\underline{x}} \right)$$

The second term in the above expression contains $\frac{1}{\eta} \sum_{\lambda=1}^{\eta} x$ which is the average value of the x deflection for all peaks and valleys sampled. According to our assumption of large η and uniform distribution, this term will be very small.

Similarly, the third through sixth terms contain average values of variables which tend toward zero with large η.

$$\sum_{\lambda=1}^{\eta} \dot{\underline{x}}\, \delta_\lambda = \frac{\eta}{\sqrt{2}\, U}\, a$$

$$a = \frac{\sqrt{2}\, U}{\eta} \sum_{\lambda=1}^{\eta} \dot{\underline{x}}\, \delta_\lambda$$

The next cross switch on the block diagram effectively creates the function $\underline{x}\ \dot{\underline{x}}\ \delta$, where $\underline{x}$ takes on values ± 1 to indicate the sign of x. For a single disagreement:

$$\underline{x}\ \dot{\underline{x}}\ \delta = \frac{1}{\sqrt{2}\,\eta} \left(a\,\underline{x} + b \left| x \right| + c\, y\, \underline{x} + d\, \dot{\underline{y}}\, \dot{\underline{x}} + e \left| x \right| \dot{\underline{y}}\, \dot{\underline{x}} + f\, y\, \dot{\underline{y}}\, \dot{\underline{x}}\, \underline{x} \right)$$

Note $\underline{x}\, x = \left| x \right|$

Summing over the frame scan, all terms except the second disappear due to uniform distribution:

$$\sum_{\lambda=1}^{\eta} \underline{x}\ \dot{\underline{x}}\ \delta_\lambda = \frac{b}{\sqrt{2}\,\eta} \sum_{\lambda=1}^{\eta} \left| x \right|$$

Letting the length of a side be ℓ the average value of $\left| x \right| = \frac{\ell}{4}$, so with uniform distribution

$$\sum_{\lambda=1}^{\eta} \left| x \right| = \frac{\eta \ell}{4}$$

$$\sum_{\lambda=1}^{\eta} \underline{x}\,\dot{\underline{x}}\,\delta_{\lambda} = \frac{b\,\ell\,n}{4\sqrt{2}\,U}$$

$$b = \frac{4\sqrt{2}\,U}{\eta\,\ell} \sum_{\lambda=1}^{\eta} \underline{x}\,\dot{\underline{x}}\,\delta_{\lambda}$$

The expressions for the other four components may be similarly derived with the following results:

$$c = \frac{4\sqrt{2}\,U}{\eta\,\ell} \sum_{\lambda=1}^{\eta} \underline{y}\,\dot{\underline{x}}\,\delta_{\lambda}$$

$$d = \frac{\sqrt{2}\,U}{\eta} \sum_{\lambda=1}^{\eta} \dot{\underline{y}}\,\delta_{\lambda}$$

$$e = \frac{4\sqrt{2}\,U}{\eta\,\ell} \sum_{\lambda=1}^{\eta} \underline{x}\,\dot{\underline{y}}\,\delta_{\lambda}$$

$$f = \frac{4\sqrt{2}\,U}{\eta\,\ell} \sum_{\lambda=1}^{\eta} \underline{y}\,\dot{\underline{y}}\,\delta_{\lambda}$$

Examining the expressions for the six components, it may be seen that each contains a sum of time intervals, a constant and a factor $\frac{1}{\eta}$. The $\frac{1}{\eta}$ factor is not included in the error signal feed back to distort the scan. Therefore, the rate of change in distortion will be a function of the number of peaks and valleys.

When the distortion loop has been closed for a sufficient number of frames to reduce the disagreement count to a minimum, the integrator outputs will be proportional to the actual distortion components without the factor of which appears in the open loop error signal.

Effects of Non-Uniform Distribution

Earlier we assumed that each of the error coefficients would be "pure", that is, in the six term sums, five terms would drop out due to uniform distribution of peaks and valleys in the four quadrants of the image.

Let us see what would happen if this were not the case. Recall the expression created by the first cross switch:

$$\sum_{\lambda=1}^{\eta} \pm \delta_{\lambda} = \frac{\eta}{\sqrt{2}\,U} \left(a + \frac{b}{\eta} \sum_{\lambda=1}^{\eta} x \quad \text{etc} \right)$$

If the amount of detail in the right half of the picture were greater than the left half $\frac{l}{\eta} \sum_{\lambda=1}^{\eta} x$ would not be zero. Let us also assume that the polarity of $\frac{b}{\eta} \sum_{\lambda=1}^{\eta} x$ is opposite from that of a but less than a. When the loop is closed, a will start to decrease because the polarity of the error term is correct. However, a will not decrease as fast as b, so the subsidiary term will tend to drop away and allow a to dominate the expression. Thus, the initial mis-weighing of the coefficient tends to correct itself.

Looking at the subsidiary terms of all six expressions, it can be seen that each contains an error coefficient multiplied by an average value of a scan variable sampled over all the peaks and valleys.

When the loop is closed to distort the scan, as long as the initial polarity of all six coefficients is correct, the system should lock in. This is because each subsidiary term contains an error coefficient which will tend to decrease. Thus, the subsidiary terms will not dominate the expressions even though the dominant terms are decreasing, as long as the rates of all six loops are matched.